

Non-commutative Cluster Lagrangians

Alexander B. Goncharov, Maxim Kontsevich

Contents

1	Introduction	2
1.1	\mathcal{Q} -diagrams of cooriented hypersurfaces	2
1.2	Lagrangians assigned to \mathcal{Q} -diagrams in surfaces and threefolds	4
1.3	\mathcal{Q} -diagrams and non-commutative cluster varieties	5
2	The basic non-commutative cluster Lagrangian	13
2.1	Non-commutative cluster Lagrangian for the basic \mathcal{Q} -diagram	13
2.2	Proof of Theorem 2.1	16
2.3	The basic non-commutative cluster Lagrangian in \mathcal{A} -coordinates	22
3	Boundaries at infinity of singular Lagrangians	27
4	Spectral covers for alternating and \mathcal{Q}-diagrams in threefolds	31
5	Cluster Lagrangians in non-commutative character varieties	34
5.1	Two flavors of cluster varieties from \mathcal{Q} -diagrams of discs	34
5.2	\mathcal{A} -coordinates from \mathcal{Q} -diagrams of discs	35
5.3	\mathcal{Q} -diagrams of discs from ideal triangulations of threefolds	37
5.4	Cluster Lagrangians in non-commutative character varieties	42
6	Appendices	43
6.1	A: Non-commutative cluster \mathcal{A} -varieties	43
6.2	B: Admissible dg-sheaves	47

Abstract

The space $\text{Loc}_m(S)$ of rank m flat bundles on a closed surface S is K_2 -symplectic. A threefold M bounding S gives rise a K_2 -Lagrangian \mathcal{L}_M in $\text{Loc}_m(S)$ given by the flat bundles on S extending to M . We generalize this, replacing the zero section in T^*M by certain singular Lagrangians in T^*M .

First, we introduce \mathcal{Q} -diagrams in threefolds. They are collections \mathcal{Q} of smooth cooriented surfaces $\{S_i\}$, intersecting transversally everywhere but in a finite set of quadruple crossing points. We require that shifting any surface S_i from such a point in the direction of its coorientation creates a simplex with the cooriented out faces. The \mathcal{Q} -diagrams are 3d analogs of bipartite ribbon graphs.

Let \mathbb{L} be the Lagrangian in T^*M given by the union of the zero section and the conormal bundles to the cooriented surfaces S_i of \mathcal{Q} . Let $\mathcal{X}_{\mathbb{L}}$ be the stack of admissible dg-sheaves \mathcal{F} on M with the microlocal support in \mathbb{L} , whose microlocalization at $T_{S_i}^*M - 0$ is a rank one local system.

We introduce the boundary $\partial\mathbb{L}$ of \mathbb{L} . It is a singular Lagrangian in a symplectic space, providing a symplectic stack $\mathcal{X}_{\partial\mathbb{L}}$, and a restriction functor $\mathcal{X}_{\mathbb{L}} \rightarrow \mathcal{X}_{\partial\mathbb{L}}$. The image of the latter is Lagrangian. We show that, under mild conditions on $\mathcal{Q} \cap \partial M$, this Lagrangian has a cluster description, and so it is a K_2 -Lagrangian. It also has a simple description in the non-commutative setting.

1 Introduction

1.1 Q-diagrams of cooriented hypersurfaces

All Lemmas in Section 1.1 are evident.

1.1.1 Q-diagrams of hypersurfaces

Let X be a manifold. A *coorientation* of a hypersurface H in X is a choice of a connected component of the conormal bundle to H minus the zero section. This component is called the conormal bundle to H . If X is oriented, a coorientation of a hypersurface is equivalent to its orientation.

Definition 1.1. *A collection of smooth cooriented hypersurfaces in an m -dimensional manifold is a Q-diagram if the intersection points where $k < m$ hypersurfaces meet are transversal intersections, and*

1. *The remaining isolated intersection points q are intersections of $m + 1$ hypersurfaces.*
2. *Shifting any of the hypersurfaces intersecting at q in the direction of its coorientation we create an m -dimensional simplex with the cooriented out faces.*

Condition (2) just means that the convex hull of the endpoints of oriented conormals h_0, \dots, h_m to the hypersurfaces intersecting at q contains zero, i.e. they satisfy a single up to a constant linear relation

$$\alpha_0 h_0 + \dots + \alpha_m h_m = 0, \quad \alpha_0, \dots, \alpha_m > 0. \tag{1}$$

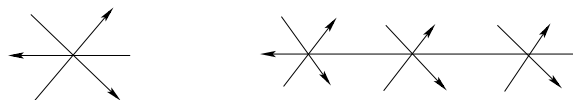


Figure 1: Q-diagrams of oriented curves on a surface are triple crossing diagrams.

Lemma 1.2. *A Q-diagram in a manifold cuts a Q-diagram on each hypersurface of the collection.*

A Q-diagram \mathcal{Q} in X provides a decomposition of $X - \mathcal{Q}$ into connected domains \mathcal{C} . A vertex $q \in \mathcal{C}$ is called *consistently cooriented* if the all faces of \mathcal{C} meeting at q are either cooriented in, or cooriented out of \mathcal{C} . A domain is *colored* if all its vertices are consistently oriented, and *mixed* if none is consistently oriented. A colored domain is a \circ -domain if its faces are cooriented in, and a \bullet -domain otherwise.

Lemma 1.3. *Given a Q-diagram \mathcal{Q} in X , every component of $X - \mathcal{Q}$ is either colored, or mixed.*

A component in $X - \mathcal{Q}$ is colored if and only if all its boundary faces are colored by the same color.

1.1.2 Alternating diagrams of hypersurfaces

A finite collection of cooriented points on a line is called an alternating diagram if traversing the line the coorientations of the points alternate.



Figure 2: Alternating diagrams of points on a line, and of oriented curves on a surface.

Definition 1.4. *An alternating diagram in a manifold X is a normal crossing connected collection \mathcal{H} of smooth cooriented hypersurfaces in X such that*

- For any intersection line in \mathcal{H} the coorientations of the hypersurfaces intersecting it alternate.

We require that an alternating diagram intersects the boundary of the manifold X transversally.

An alternating diagram on X does not necessarily induce an alternating diagram on the boundary. The following Lemma provides an equivalent inductive definition.

Lemma 1.5. *Under the same assumptions as in Definition 1.4, an \mathcal{H} is an alternating diagram if intersecting the collection with any of its hypersurfaces H we get an alternating diagram in H .*

We define colored and mixed domains for alternating diagrams the same way as for \mathcal{Q} -diagrams. Lemma 1.3 holds for alternating diagrams, see Figure 3:

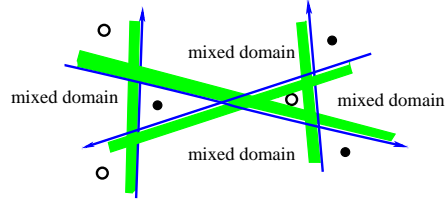


Figure 3: (Co)oriented lines and \bullet , \circ and mixed domains for an alternating diagram.

1.1.3 \mathcal{Q} -diagrams \longrightarrow alternating diagrams.

A \mathcal{Q} -diagram gives rise to an alternating diagram: we resolve each isolated intersection point q by moving any hypersurface containing q in the direction of its coorientation. This way we get an equivalence

$$\{\mathcal{Q}\text{-diagrams}\} \longleftrightarrow \{\text{Alternating diagrams whose } \bullet\text{-domains are simplices}\}. \quad (2)$$

Indeed, shrinking the \bullet -domains to points we get a \mathcal{Q} -diagram.

Lemma 1.6. *Let q be an isolated intersection point of a \mathcal{Q} -diagram \mathcal{Q} . Then the hypersurfaces of \mathcal{Q} induce an alternating collection on the boundary of a little sphere S_q around q .*

1.1.4 \mathcal{Q} -diagrams, alternating diagrams, and bipartite graphs on surfaces

Here are the basic facts concerning this, following [GKe, Sections 2.2, 2.3, 2.6].

1. By definition, \mathcal{Q} -diagrams on a surface S are the same as *triple crossing diagrams* on S [Th].¹

$$\{\mathcal{Q}\text{-diagrams on a surface } S\} = \{\text{triple crossing diagrams on a surface } S\}. \quad (3)$$



Figure 4: Resolving triple crossings we get a bipartite graph.

¹D. Thurston considered triple crossing diagrams only in a disc.

2. A *zig-zag strand* on a bipartite surface graph is a path on the graph turning left at the \bullet -vertices, and right at the \circ -vertices. Assigning to a bipartite surface graph the collection of its zig-zag strands pushed out of the vertices provides an equivalence

$$\begin{aligned} \{\text{minimal bipartite graphs on a surface } S\} = \\ \{\text{minimal alternating diagrams on } S \text{ with contractible colored domains}\}. \end{aligned} \quad (4)$$

3. Any bipartite graph can be transformed to a one with 3-valent \bullet -vertices by splitting the \bullet -vertices of valency > 3 by adding edges, and introducing 2-valent \circ -vertices in the middle of these edges.

Given a collection of zig-zags strands for a bipartite surface graph Γ with 3-valent \bullet -vertices, draw zig-zag strands assigned to all edges of Γ , as on Figure 4. Then each vertex of Γ is surrounded by an oriented polygon of arcs. Shrink the clockwise triangles near the \bullet -vertices to points, getting a triple crossing diagram. This way we get an equivalence

$$\begin{aligned} \{\text{minimal bipartite graphs on a surface } S \text{ with 3-valent } \bullet\text{-vertices}\} = \\ \{\text{minimal triple crossing diagrams on } S \text{ with contractible } \circ\text{-domains}\}. \end{aligned} \quad (5)$$

We conclude that

- *Alternating diagrams on surfaces are slightly more general geometric objects than bipartite graphs and triple crossing diagrams.*
- *\mathcal{Q} -diagrams in threefolds are 3d analogs of bipartite graphs / triple crossing diagrams on surfaces.*

1.2 Lagrangians assigned to \mathcal{Q} -diagrams in surfaces and threefolds

We start from general definitions. Recall that a coorientation of a hypersurface H in a manifold X is a section of the bundle of conormal rays $(T^*X - 0)/\mathbb{R}_{>0}^\times$. This section is the Legendrian of the cooriented hypersurface. The *conormal bundle* Lagrangian T_H^*X is its preimage in $T^*X - 0$.

Definition 1.7. *Let \mathcal{H} be a finite collection $\{H_i\}$ of smooth cooriented hypersurfaces with disjoint Legendrians in a manifold X . It gives rise to the following Lagrangian in T^*X :*

$$\mathbb{L} = \mathbb{L}_{\mathcal{H}} := \text{the union of the zero section } X^\circ \text{ and the conormal bundles } T_{H_i}^*X \text{ to } H_i. \quad (6)$$

1.2.1 Lagrangians and spectral surfaces assigned to alternating diagrams on surfaces

Definition 1.8. *Let \mathcal{T} be an alternating diagram on a surface. Consider the following Lagrangian subset:*

$$\mathbb{L}^\circ = \mathbb{L}_{\mathcal{T}}^\circ := \mathbb{L}_{\mathcal{T}} - \{\text{the union of zero sections for mixed domains}\}. \quad (7)$$

Lemma 1.9. *The Lagrangian $\mathbb{L}_{\mathcal{T}}^\circ$ is homeomorphic to a smooth surface $\Sigma_{\mathcal{T}}$, called the spectral surface:*

$$\mathbb{L}_{\mathcal{T}}^\circ = \Sigma_{\mathcal{T}}. \quad (8)$$

The loops of the diagram \mathcal{T} are identified with the boundary circles on the spectral surface.

Proof. Let us describe the spectral surface. Take a disjoint collection of domains \mathcal{D}'_* matching the colored domains \mathcal{D}_* of $S - \mathcal{T}$. For each intersection point e on \mathcal{T} there are two colored domains \mathcal{D}_\bullet and \mathcal{D}_\circ sharing the e . Denote by \mathcal{D}'_\bullet and \mathcal{D}'_\circ disjoint copies of these domains. Glue them along a bridge replacing the intersection point, with the twist by 180° , getting a smooth surface denoted $\Sigma_{\mathcal{T}}$. Then, just as, say, in [GKo], we get a homeomorphism (8). \square

The Lagrangian \mathbb{L}° for a triple crossing diagram on a surface is Hamiltonian isotopic to the one for the associated alternating diagram. In particular, it is non-singular.

Example. Assume that colored domains of $S - \mathcal{T}$ are contractible. Let Γ be the bipartite ribbon graph assigned to \mathcal{T} in (5). Let Γ^* be the conjugate bipartite ribbon graph, obtained by reversing the cyclic order of edges at the \bullet -vertices of Γ [GKe], and S_{Γ^*} the associated surface glued from the ribbons of Γ^* . Then the spectral surface $\Sigma_{\mathcal{T}}$ is the surface S_{Γ^*} , and

$$\{\text{zig-zag loops on } \Gamma\} = \{\text{boundary loops on } \Gamma^*\} = \{\text{boundary circles on } \Sigma_{\mathcal{T}}\}. \quad (9)$$

1.2.2 Lagrangians and spectral threefolds assigned to \mathcal{Q} -diagrams in threefolds

Definition 1.10. *Given a \mathcal{Q} -diagram in a threefold M , consider the Lagrangian subset*

$$\mathbb{L}_{\mathcal{Q}}^\circ := \mathbb{L}_{\mathcal{Q}} - \{\text{the union of zero sections for mixed domains}\}. \quad (10)$$

The Lagrangian $\mathbb{L}_{\mathcal{Q}}^\circ$ has singularities at the quadruple intersection points. Denote by $\text{Sing}(\mathbb{L}_{\mathcal{Q}}^\circ)$ the set of singularities. The *link* of any singular point of $\mathbb{L}_{\mathcal{Q}}^\circ$ is the intersection of $\mathbb{L}_{\mathcal{Q}}^\circ$ with a small sphere around the point. Each quadruple intersection point q of \mathcal{Q} gives rise to a point q_\circ of $\mathbb{L}_{\mathcal{Q}}^\circ$ given by the zero cotangent vector at q .

Lemma 1.11. *The projection $T^*M \rightarrow M$ induces a bijection*

$$\text{Sing}(\mathbb{L}_{\mathcal{Q}}^\circ) \xrightarrow{\sim} \{\text{the points } q_\circ \text{ for all quadruple intersection points of } \mathcal{Q}\}. \quad (11)$$

The link of a singular point of $\mathbb{L}_{\mathcal{Q}}^\circ$ is homeomorphic to a torus, equipped with an action of the group A_4 .

Proof. The complement to quadruple intersection points is locally isomorphic to a transversal intersection of two planes in \mathbb{R}^3 . So the first claim follows from Lemma 1.9. The second is proved in Lemma 2.2. \square

Let us remove a small ball B_q around each quadruple intersection points q of \mathcal{Q} . We get a threefold M_\times with the induced collection of surfaces $\mathcal{Q}_\times \subset M_\times$. It gives rise to a Lagrangian $\mathbb{L}_\times \subset T^*M_\times$, as well as its closed subset \mathbb{L}_\times° obtained by removing zero sections over all mixed domains in $M_\times - \mathcal{Q}_\times$.

Lemma 1.12. *The Lagrangian \mathbb{L}_\times° is a smooth threefold with boundary.*

Proof. The diagram \mathcal{Q}_\times is locally a product of an interval and a cooriented coordinate cross. So we can apply the 3d version of the construction from the proof of Lemma 1.9. Take a disjoint collection of the 3d domains \mathcal{D}'_* matching the colored domains \mathcal{D}_* of $M - \mathcal{Q}$. For each intersection edge e on \mathcal{Q} there are two colored domains \mathcal{D}_\bullet and \mathcal{D}_\circ sharing the edge e . Denote by \mathcal{D}'_\bullet and \mathcal{D}'_\circ their disjoint copies. Glue them with the twist by 180° , getting a smooth threefold. \square

Definition 1.13. *The threefold with boundary \mathbb{L}_\times° is the spectral threefold $\Sigma_{\mathcal{Q}}$ for the \mathcal{Q} -diagram \mathcal{Q} .*

The boundary $\partial\mathbb{L}_\times^\circ$ of the Lagrangian threefold \mathbb{L}_\times° assigned to a \mathcal{Q} -diagram of cooriented surfaces $\{S_i\}$ in a threefold M with its own boundary ∂M plays the crucial role in the story. It is again a Lagrangian in a germ of a symplectic manifold. We give a general definition of the boundary of a Lagrangian with mild singularities in Section 3. The boundary $\partial\mathbb{L}_\times^\circ$ is described in Section 1.3.5.

Let us now explain how we associate various stacks to the Lagrangians assigned to \mathcal{Q} -diagrams.

1.3 \mathcal{Q} -diagrams and non-commutative cluster varieties

A manifold X with boundary ∂X gives rise to the dg-stack of local systems $\text{Loc}(X)$ and the restriction functor $\text{Loc}(X) \rightarrow \text{Loc}(\partial X)$, whose image is a shifted derived Lagrangian. One can replace manifolds by singular Lagrangian subsets with "tame" singularities in symplectic manifolds, and get a similar picture. We start from the general set-up, and then proceed to Lagrangians corresponding to \mathcal{Q} -diagrams, which in the case when X is a surface or a threefold provide the non-commutative cluster variant of the story.

1.3.1 Categories and stacks assigned to singular Lagrangians.

A closed Lagrangian subset L with "tame" singularities in a symplectic manifold gives rise to a sheaf of categories \mathfrak{C}_L on L , depending only on the germ of ambient symplectic manifold at L , see [K], [N], [GPS1]-[GPS3]. The section of the sheaf \mathfrak{C}_L over an open subset U of L which can be smoothified to a manifold is equivalent to the category of complexes of local systems on U . Another example: let \mathcal{E}_n be a single vertex graph with n cyclically ordered edges. Then the section of the sheaf \mathfrak{C}_L over an open subset isomorphic to a product of a disc and the graph \mathcal{E}_n is the derived category of representations of the quiver of type A_{n-1} .

There is a Lagrangian ∂L of dimension one less than L , called the *boundary of infinity* of L , or just the *boundary* of L , living in a germ of a symplectic manifold \mathcal{S} , see Section 3, and the restriction functor:

$$\text{Res} : \mathfrak{C}_L \longrightarrow \mathfrak{C}_{\partial L}. \quad (12)$$

From now on, L is a closed conical Lagrangian subset in the cotangent bundle T^*X to a manifold X . Then the category \mathfrak{C}_L can be described in terms of the category $D_L^b(X)$ of complexes of constructible sheaves on X with the microlocal support in L , twisted by a $\mathbb{Z}/2\mathbb{Z}$ -gerb with the second Stiefel-Whitney class $w_2[T^*X] \in H^2(X, \mathbb{Z}/2\mathbb{Z})^2$ [KS], [GKS]. This description uses the microlocalisation functor [KS]

$$\mu : D_L^b(X) \longrightarrow D^b(L).$$

Below, given a skew field R , we consider as the base category the category of complexes of constructible R -sheaves on X , referred below just as sheaves. We denote by $\mathfrak{C}_L(L)$ the category of global sections of the sheaf of categories \mathfrak{C}_L on L .

Let \mathcal{H} be a collection of smooth cooriented hypersurfaces $\{H_i\}$ in X . The assigned in (6) Lagrangian $\mathbb{L} = \mathbb{L}_{\mathcal{H}}$ in T^*X gives rise to the subcategory $\mathfrak{C}_L^{(1)}(\mathbb{L}) \subset \mathfrak{C}_L(L)$, given by the sheaves \mathcal{F} on X such that:

$$\begin{aligned} & \text{For each cooriented hypersurface } H_i \text{ of } \mathcal{H}, \text{ the microlocalization of the sheaf } \mathcal{F} \\ & \text{at the punctured conormal bundle } T_{H_i}^*X - \{\text{zero section}\} \text{ is an } R\text{-rank one local system.} \end{aligned} \quad (13)$$

The category $\mathfrak{C}_L^{(1)}(\mathbb{L})$ contains the subcategory \mathcal{C}_L of \mathcal{H} -admissible sheaves on X [GKo], see Section 6.2. Similar categories for surfaces, in the commutative set up, were studied in [STZ], [STWZ], [STW].

An *admissible deformation* of the collection \mathcal{H} is a deformation keeping the hypersurfaces smooth and their Legendrians disjoint, while the intersection pattern can change. The category of \mathcal{H} -admissible sheaves is invariant under admissible deformations: this was proved when X is a surface in [GKo], and the proof is easily extended to the crucial for us case when X is a threefold.

Definition 1.14. *Denote by $[\mathcal{H}]$ the admissible deformation class of \mathcal{H} . We denote by $\mathcal{X}_L = \mathcal{X}_{[\mathcal{H}]}$ the derived stack of objects in \mathcal{C}_L , and by $\mathcal{X}_{\partial L}$ the derived stack of objects in $\mathcal{C}_{\partial L}$.*

The restriction functor (12) induces a map of derived stacks

$$\text{Res} : \mathcal{X}_L \longrightarrow \mathcal{X}_{\partial L}. \quad (14)$$

1.3.2 Main results.

When the manifolds X are surfaces and threefolds with boundary, the stacks $\mathcal{X}_{[\mathcal{H}]}$ together with the restriction functors (14) give rise to non-commutative cluster structures of various types. Their clusters are provided by the \mathcal{Q} -diagrams in the same admissible deformation class. Precisely:

²We can twist \mathfrak{C}_L by any \mathbb{G}_m -gerb. If we use for the twist the pull back of $w_2(X)$ by the natural map $L \longrightarrow X$, we get the usual category of constructible sheaves.

- Let S be a smooth surface with boundary, and \mathcal{T} an alternating diagram on S . Then the stack $\mathcal{X}_{[\mathcal{T}]}$ carries a non-commutative cluster Poisson structure [GKo], generalising cluster Poisson varieties assigned to \mathcal{T} in the commutative setting [GKe]. The restriction functor (14) describes its symplectic leaves. The clusters are given by the non-commutative tori of flat line bundles on spectral surfaces $\Sigma_{\mathcal{T}}$. If the boundary of the surface S is empty, we get a K_2 -symplectic stack $\mathcal{X}_{[\mathcal{T}]}$.
- For threefolds M with boundary, the image of the restriction functor is a non-commutative cluster Lagrangian $\mathcal{L}_{[\mathcal{Q}]}$. The adjective *cluster* means that we describe it in an explicit and uniform way. In the commutative case we get cluster K_2 -Lagrangians. The clusters are given by the Lagrangians $\mathcal{L}_{\mathcal{Q}}$ assigned to \mathcal{Q} -diagrams \mathcal{Q} in the given admissible deformation class $[\mathcal{Q}]$, which intersect the boundary by an alternating diagram \mathcal{T} . Precisely, we define a smooth closed surface $\Upsilon_{\mathcal{Q}}$ by gluing the surfaces of the collection \mathcal{Q} with the spectral surface $\Sigma_{\mathcal{T}}$ of \mathcal{T} . Then $\mathcal{L}_{\mathcal{Q}}$ is an explicitly described Lagrangian in the non-commutative torus of flat R -line bundles on the surface $\Upsilon_{\mathcal{Q}}$:

$$\mathcal{L}_{\mathcal{Q}} \subset \text{Loc}_1(\Upsilon_{\mathcal{Q}}). \quad (15)$$

If all surfaces of the collection \mathcal{Q} are discs, then $\Upsilon_{\mathcal{Q}}$ is the compactified spectral surface $\Sigma_{\mathcal{T}}$.

In the commutative case the K_2 -symplectic structure of the cluster variety $\mathcal{X}_{[\mathcal{T}]}$ provides, by applying the Beilinson-Deligne *symbole modéré*, a line bundle with connection on the cluster variety, whose restriction to the cluster Lagrangian $\mathcal{L}_{\mathcal{Q}}$ is canonically trivialised.

Here is an example. Take a threefold M and a set of points $\{p_1, \dots, p_n\}$ on its boundary ∂M . We construct \mathcal{Q} -diagrams of discs in M describing the cluster nature of the stack of flat m -dimensional R -vector bundles on the punctured surface $\partial M - \{p_1, \dots, p_n\}$ with the following properties:

They have unipotent monodromies around the punctures p_i , carry monodromy invariant flags near the punctures, and can be extended to M .

1.3.3 Why \mathcal{Q} -diagrams, rather than alternating diagrams?

Let \mathcal{H} be an alternating diagram of cooriented surfaces obtained by resolution of the quadruple intersection points of a \mathcal{Q} -diagram. Then we have canonical equivalences of stacks

$$\mathcal{X}_{[\mathcal{H}]} = \mathcal{X}_{[\mathcal{Q}]}. \quad (16)$$

The singular set of the Lagrangian subset $\mathbb{L}_{\mathcal{H}}^{\circ}$ consists of the points t_{\circ} assigned to the triple intersection points t of \mathcal{H} . However the link of a singular point t_{\circ} is a *surface with boundary* - a pair of pants, rather than a torus from Lemma 1.11. So, although we can define the stacks $\mathcal{X}_{\mathcal{H}}^{\circ}$ for alternating diagrams of surfaces, they are meaningless: the admissible sheaves vanishing on mixed domains are forced to have the zero microlocalization on the punctured cotangent bundles to the surfaces.³

Therefore we do not get a cluster cover of the Lagrangian $\mathbb{L}_{\mathcal{H}}$ directly from alternating diagrams.

This is why we deal with \mathcal{Q} - diagrams of surfaces rather than with the related alternating diagrams.

1.3.4 Non-commutative cluster Poisson varieties from alternate diagrams on surfaces.

Let \mathcal{T} be an alternating diagram on a surface S . Recall the Lagrangian $\mathbb{L}_{\mathcal{T}}$ assigned to \mathcal{T} in (6). The stack $\mathcal{X}_{[\mathcal{T}]}$ parametrises admissible dg-sheaves \mathcal{F} on S with the microlocal support in $\mathbb{L}_{\mathcal{T}}$ satisfying condition (13). It carries a non-commutative cluster Poisson structure. Restriction functor (14) describes its symplectic leaves. Let us describe the clusters.

Definition 1.15. *Denote by $\mathcal{X}_{\mathcal{T}}^{\circ}$ the substack of stack $\mathcal{X}_{[\mathcal{T}]}$ parametrising objects vanishing on mixed domains for the alternating diagram \mathcal{T} . So their microlocal supports are contained in the Lagrangian $\mathbb{L}_{\mathcal{T}}^{\circ}$.*

³The category assigned to a closed Lagrangian subset in the vicinity of a (single vertex ribbon graph with n edges) $\times \mathbb{R}^m$ is equivalent to the derived category of representations of the quiver A_n , see [K], [GPS1]-[GPS3]. So near the boundary of a surface we get the category of representations of A_0 -quiver, which consists of the single object: the zero.

Recall the spectral surface $\Sigma_{\mathcal{T}}$ for the alternating diagram \mathcal{T} from Lemma 1.9. Let $\text{Loc}_1(\Sigma_{\mathcal{T}})$ be the non-commutative tori parametrising the R -rank one local systems on the surface $\Sigma_{\mathcal{T}}$. Thanks to (8),

$$\mathcal{X}_{\mathcal{T}}^{\circ} = \text{Loc}_1(\Sigma_{\mathcal{T}}). \quad (17)$$

The intersection form on the spectral surface gives rise to a non-commutative Poisson structure on $\mathcal{X}_{\mathcal{T}}^{\circ}$. The isotopy classes of alternating diagrams \mathcal{T} in a given admissible deformation class provide cluster Poisson tori (17), defining the non-commutative cluster Poisson structure on the stack $\mathcal{X}_{[\mathcal{T}]}$. Modifications $\mathcal{T} \rightarrow \mathcal{T}'$, called *two by two moves*, provide birational isomorphisms of non-commutative Poisson tori

$$\text{Loc}_1(\Sigma_{\mathcal{T}}) \rightarrow \text{Loc}_1(\Sigma_{\mathcal{T}'}). \quad (18)$$

We conclude that:

The stack $\mathcal{X}_{[\mathcal{T}]}$ assigned to an alternating diagram \mathcal{T} on a surface carries a structure of a non-commutative cluster Poisson variety. Its cluster tori are the tori (17) provided by the alternate diagrams admissibly equivalent to \mathcal{T} . The restriction functor (14) describes its symplectic leaves. The birational maps (18) generate the cluster Poisson transformations.

1.3.5 Cluster Lagrangians from \mathcal{Q} -diagrams in threefolds.

Let M be a threefold, possibly with boundary, and $\mathcal{Q} = \{S_i\}$ a \mathcal{Q} -diagram of smooth cooriented surfaces in M transversal to the boundary ∂M . Recall the Lagrangian $\mathbb{L} = \mathbb{L}_{\mathcal{Q}}$ assigned to \mathcal{Q} in (6). In Section 3 we define its boundary at infinity

$$\partial\mathbb{L} \subset \mathcal{S}.$$

It is a singular Lagrangian subset $\partial\mathbb{L}$ of the dimension one less than \mathbb{L} in a certain symplectic space \mathcal{S} . It gives rise to a derived symplectic stack $\mathcal{X}_{\partial\mathbb{L}}$ and the restriction map

$$\text{Res} : \mathcal{X}_{\mathbb{L}} \rightarrow \mathcal{X}_{\partial\mathbb{L}}. \quad (19)$$

The image of the map (19) is a derived Lagrangian.

Recall the Lagrangian subset $\mathbb{L}_{\mathcal{Q}}^{\circ} \subset T^*M$ from Definition 1.16.

Definition 1.16. *Given a \mathcal{Q} -diagram in a threefold M , let $\mathcal{X}_{\mathcal{Q}}^{\circ}$ the substack of $\mathcal{X}_{\mathbb{L}}$ parametrising the objects with the microlocal supports in the Lagrangian $\mathbb{L}_{\mathcal{Q}}^{\circ}$.*

We denote by $\partial\mathbb{L}_{\mathcal{Q}}^{\circ}$ the boundary of the Lagrangian $\mathbb{L}_{\mathcal{Q}}^{\circ}$, and by $\mathcal{X}_{\partial\mathbb{L}_{\mathcal{Q}}^{\circ}}^{\circ}$ the stack of objects corresponding to the Lagrangian $\partial\mathbb{L}_{\mathcal{Q}}^{\circ}$. Our next goal is to describe the Lagrangian $\partial\mathbb{L}_{\mathcal{Q}}^{\circ}$ and the stack $\mathcal{X}_{\partial\mathbb{L}_{\mathcal{Q}}^{\circ}}^{\circ}$.

Let us assume from now on that the \mathcal{Q} -diagram $\mathcal{Q} = \{S_i\}$ intersects the boundary ∂M transversally by an alternating collection $\mathcal{T} = \{\alpha_{ij}\}$ of loops in ∂M . Then there is the spectral surface $\Sigma_{\mathcal{T}}$, see (8). It is a smooth surface, whose boundary is identified with the disjoint union of loops α_{ij} . Indeed, the loops of the alternating diagram $\partial\mathcal{Q}$ become the boundary circles on the spectral surface.⁴ The boundary of each surface S_i is a disjoint union of the loops α_{i*} . So:

$$\partial\Sigma_{\mathcal{T}} = \coprod_j \alpha_{ij} = \coprod_i \partial S_i. \quad (20)$$

Definition 1.17. *The surface $\Upsilon = \Upsilon_{\mathcal{Q}}$ is the smooth closed surface obtained by gluing the disjoint union of the surfaces S_i with the spectral surface $\Sigma_{\mathcal{T}}$ over the matching boundary components, see Figure 5:*

$$\Upsilon_{\mathcal{Q}} = \Upsilon := \left(\coprod_i S_i \right) *_{\{\alpha_{ij}\}} \Sigma_{\mathcal{T}}. \quad (21)$$

⁴See Lemma 1.9 and (9), describing the case when $\partial\mathcal{Q}$ comes from a bipartite graph.

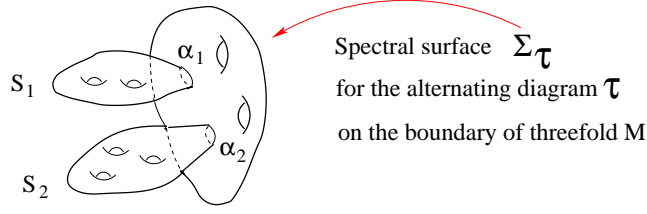


Figure 5: The surface Υ is obtained by gluing surfaces S_i to the spectral surface $\Sigma_{\mathcal{T}}$ along the loops α_{i*} .

Proposition 1.18. *The Lagrangian $\partial\mathbb{L}_{\mathcal{Q}}^{\circ} \subset S_{\mathcal{Q}}^{\circ}$ is isomorphic to the zero section Lagrangian $\Upsilon \subset T^*\Upsilon$:*

$$\partial\mathbb{L}_{\mathcal{Q}}^{\circ} = \Upsilon; \quad S_{\mathcal{Q}}^{\circ} = T^*\Upsilon.$$

The symplectic stack $\mathcal{X}_{\partial\mathbb{L}}^{\circ}$ is the non-commutative symplectic torus of flat line bundles on the surface Υ :

$$\mathcal{X}_{\partial\mathbb{L}}^{\circ} = \text{Loc}_1(\Upsilon). \quad (22)$$

The category $\mathcal{C}_{\partial\mathbb{L}}$ is the fibered product of the categories $\prod_i \text{Loc}_1(S_i)$ and $\mathcal{C}_{\mathcal{T}}$ over $\text{Loc}_1(\{\alpha_{ij}\})$:

$$\mathcal{C}_{\partial\mathbb{L}} = \prod_i \text{Loc}_1(S_i) \times_{\text{Loc}_1(\{\alpha_{ij}\})} \mathcal{C}_{\mathcal{T}}. \quad (23)$$

Let us describe the restriction functor

$$\text{Res}_{\partial\mathbb{L}} : \mathcal{X}_{\mathbb{L}} \longrightarrow \prod_i \text{Loc}_1(S_i) \times_{\text{Loc}_1(\{\alpha_{ij}\})} \mathcal{X}_{[\mathcal{T}]}. \quad (24)$$

Assigning to an admissible sheaf the flat R -line bundle on S_i given by the restriction of its microlocalisation to $T_{S_i}^*M - \{\text{zero section}\}$ we get a functor $\text{Res}_{\infty} : \mathcal{X}_{\mathbb{L}} \longrightarrow \prod_i \text{Loc}_1(S_i)$. The restriction to the boundary provides a functor $\text{Res}_{\partial M} : \mathcal{X}_{\mathbb{L}} \longrightarrow \mathcal{X}_{[\mathcal{T}]}$. Combining the two functors, we get the functor (24).

Restricting the functor $\text{Res}_{\partial M}$ to the sheaves vanishing on mixed domains we get a functor

$$\text{Res}_{\partial M}^{\circ} : \mathcal{X}_{\mathcal{Q}}^{\circ} \longrightarrow \mathcal{X}_{\mathcal{T}}^{\circ} \stackrel{(17)}{=} \text{Loc}_1(\Sigma_{\mathcal{T}}). \quad (25)$$

So we arrive at the restriction functor

$$\begin{aligned} \text{Res}_{\partial\mathbb{L}}^{\circ} : \mathcal{X}_{\mathbb{L}}^{\circ} &\longrightarrow \mathcal{X}_{\partial\mathbb{L}}^{\circ} \stackrel{(22)}{=} \text{Loc}_1(\Upsilon) \\ &\stackrel{(21)}{=} \prod_i \text{Loc}_1(S_i) \times_{\text{Loc}_1(\{\alpha_{ij}\})} \text{Loc}_1(\Sigma_{\mathcal{T}}). \end{aligned} \quad (26)$$

The images of stacks $\mathcal{X}_{\mathbb{L}}^{\circ}$ and $\mathcal{X}_{\mathbb{L}}$ under restriction functors (26) and (24) are Lagrangians, denoted by:

$$\begin{aligned} \mathcal{L}_{\mathcal{Q}}^{\circ} &:= \text{Res}_{\partial\mathbb{L}}^{\circ}(\mathcal{X}_{\mathbb{L}}^{\circ}) \subset \text{Loc}_1(\Upsilon). \\ \mathcal{L}_{[\mathcal{Q}]} &:= \text{Res}_{\partial\mathbb{L}}(\mathcal{X}_{\mathbb{L}}) \subset \prod_i \text{Loc}_1(S_i) \times_{\text{Loc}_1(\{\alpha_{ij}\})} \mathcal{X}_{[\mathcal{T}]}. \end{aligned} \quad (27)$$

The stacks $\mathcal{X}_{\mathbb{L}}$, $\mathcal{X}_{\partial\mathbb{L}}$ and the restriction map do not change under admissible deformations. However admissible deformations may not preserve intersection patterns of surfaces, and hence \mathcal{Q} -diagrams. The Lagrangians $\mathbb{L}_{\mathcal{Q}}^{\circ}$ and $\partial\mathbb{L}_{\mathcal{Q}}^{\circ}$ and the related stacks $\mathcal{X}_{\mathbb{L}}^{\circ}$ and $\mathcal{X}_{\partial\mathbb{L}}^{\circ}$ depend on the choice of a \mathcal{Q} -diagram \mathcal{Q} . Admissible deformations of \mathcal{Q} may lead to different isotopy classes of the alternating diagram \mathcal{T} on the boundary, altering the spectral surface associated with \mathcal{T} .

Therefore the \mathcal{Q} -diagrams in M in a given admissible deformation class, considered up to isotopy, give rise to a cover of the space $\mathcal{X}_{\partial\mathbb{L}}$ by Zariski open split tori $\mathcal{X}_{\partial\mathbb{L}}^{\circ}$. They are the cluster symplectic tori,

defining a cluster symplectic structure on $\mathcal{X}_{\partial\mathbb{L}}$.⁵ The subvarieties $\text{Res}_{\partial\mathbb{L}}^{\circ}(\mathcal{X}_{\mathbb{L}}^{\circ})$ form a Zariski open cover of the Lagrangian $\text{Res}_{\partial\mathbb{L}}(\mathcal{X}_{\mathbb{L}})$ in $\mathcal{X}_{\partial\mathbb{L}}$. We call the obtained structure a *cluster Lagrangian*.

Theorem 1.19. *Let \mathcal{Q} be a \mathcal{Q} -diagram in a threefold M intersecting the boundary transversally by an alternating diagram \mathcal{T} . Then $\mathcal{L}_{[\mathcal{Q}]}$ is a non-commutative cluster Lagrangian. It contains a collection of open Lagrangians $\mathcal{L}_{\mathcal{Q}}^{\circ}$ - the clusters - parametrised by the \mathcal{Q} -diagrams \mathcal{Q} in the same admissible deformation class. They are described by systems of equations, depending uniformly on the cluster.*

Theorem 1.19 is deduced from the crucial Theorem 2.1 below. We conclude that:

*\mathcal{Q} -diagrams in threefolds are a geometric source of non-commutative cluster Lagrangians.
In the commutative setting, they are a geometric source of K_2 -Lagrangians.*

Let us now describe the restriction map (26) and its image.

1. We start with the simplest, and at the same time most basic example, when M is a cube C . The 1-skeleton of the cube boundary ∂C has a unique up to a cube rotation structure of a bipartite graph Γ_C , with the \bullet and \circ vertices. We define the \mathcal{Q} -diagram \mathcal{Q}_C as the collection of four planes passing through the center of the cube, perpendicular to the cube diagonals, and cooriented $\circ \rightarrow \bullet$.

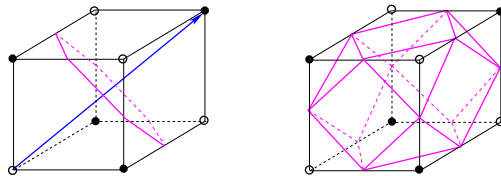


Figure 6: The diagram \mathcal{Q}_C is the union of four central plane sections perpendicular to the cube diagonals.

We give an explicit description of the Lagrangian $\text{Res}(\mathcal{X}_{\mathbb{L}_C^{\circ}})$ in Theorem 2.1, and an alternative description in Theorem 2.7.

2. In general, the key fact is that intersecting a \mathcal{Q} -diagram with a small ball B_q around any quadruple intersection points q we get a \mathcal{Q} -diagram isomorphic to \mathcal{Q}_C . Removing all balls B_q we get a threefold M_{\times} with the induced collection of cooriented surfaces $\mathcal{Q}_{\times} \subset M_{\times}$. It gives rise to a Lagrangian $\mathbb{L}_{\times} \subset T^*M_{\times}$, as well as its closed subset $\mathbb{L}_{\times}^{\circ}$ obtained by removing zero sections over all mixed domains in $M_{\times} - \mathcal{Q}_{\times}$.

Lemma 1.20. *The Lagrangian $\mathbb{L}_{\times}^{\circ}$ is a smooth threefold with boundary. Its boundary $\partial\mathbb{L}_{\times}^{\circ}$ is isomorphic to the disjoint union of the surface Υ and the cube surfaces ∂C_{q_i} for all quadruple intersection points q :*

$$\partial\mathbb{L}_{\times}^{\circ} = \Upsilon \cup \partial C_{q_1} \cup \dots \cup \partial C_{q_m}. \quad (28)$$

Proof. The diagram \mathcal{Q}_{\times} is locally a product of an interval and a cooriented coordinate cross. So we can apply the 3d version of the construction from the proof of Lemma 1.9. Precisely, take a disjoint collection of the 3d domains \mathcal{D}'_* matching the colored domains \mathcal{D}_* of $M - \mathcal{Q}$. For each intersection edge e on \mathcal{Q} there are two colored domains \mathcal{D}_{\bullet} and \mathcal{D}_{\circ} sharing the edge e . Denote by \mathcal{D}'_{\bullet} and \mathcal{D}'_{\circ} their disjoint copies. Glue them along a bridge replacing the intersection edge, with the twist by 180° , getting a smooth threefold denoted $\Sigma_{\mathcal{Q}}$. Then we get the first claim. The second claim is clear. \square

Definition 1.21. *The threefold with boundary $\mathbb{L}_{\times}^{\circ}$ is the spectral threefold $\Sigma_{\mathcal{Q}}$ for the \mathcal{Q} -diagram \mathcal{Q} .*

Next, let N be any threefold with boundary S . Then, in the commutative case, the intersection pairing on S provides the canonical element

$$W_N \in \mathcal{O}^{\times}(\text{Loc}_1(S)) \wedge \mathcal{O}^{\times}(\text{Loc}_1(S)). \quad (29)$$

⁵Note that since ∂M has no boundary, the surface $\partial\mathbb{L}^{\circ}$ are closed, and the related cluster Poisson stacks are symplectic.

Lemma 1.22. *The restriction of the element W_N to the subspace $\text{Loc}_1(S, N)$ of $\text{Loc}_1(S)$ given by the line bundles on S which extend to N is equal to zero.*

Proof. Follows from the fact that the image of the restriction map $H^1(N; \mathbb{Z}) \rightarrow H^1(\partial N; \mathbb{Z})$ is Lagrangian for the \cup -pairing on $H^1(S; \mathbb{Z})$. \square

Recall the map

$$\begin{aligned} d \log : \mathcal{O}^\times(\text{Loc}_1(S)) \wedge \mathcal{O}^\times(\text{Loc}_1(S)) &\longrightarrow \Omega_{\log}^2(\text{Loc}_1(S)), \\ d \log : f \wedge g &\longrightarrow d \log(f) \wedge d \log(g). \end{aligned} \tag{30}$$

The element W_N provides the K_2 -symplectic structure $d \log(W_N)$ on $\text{Loc}_1(S)$. By Lemma 1.22 the subspace $\text{Loc}_1(S, N)$ is a K_2 -Lagrangian.

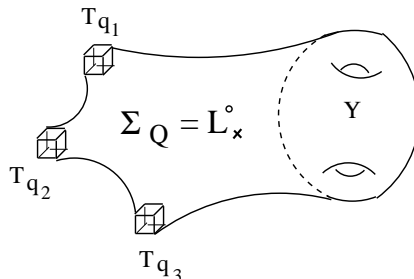


Figure 7: Spectral threefold $\Sigma_Q = \mathbb{L}_x^\circ$. Its boundary is disjoint union of the closed surface Υ , see Figure 5, and tori T_{q_i} . The torus T_q is the spectral surfaces for the bipartite graph on the cube surface C_q .

Applying this to the spectral threefold $\Sigma_Q = \mathbb{L}_x^\circ$, and using (28), we get a K_2 -Lagrangian

$$\Lambda_Q \subset \text{Loc}_1(\Upsilon) \times \prod_q \text{Loc}_1(\partial C_q).$$

In Theorem 2.7 we describe the basic K_2 -Lagrangian $\mathcal{L}_{C_q} \subset \text{Loc}_1(C_q)$. Their product is a K_2 -Lagrangian

$$\mathcal{L}_C := \prod_q \mathcal{L}_{C_q} \subset \prod_q \text{Loc}_1(C_q).$$

We consider Λ_Q as a K_2 -Lagrangian correspondence between the K_2 -symplectic varieties $\text{Loc}_1(\Upsilon)$ and $\prod_q \text{Loc}_1(\partial C_q)$. Applying it to the K_2 -Lagrangian \mathcal{L}_C we get the K_2 -Lagrangian we were looking for:

$$\Lambda_Q \circ \mathcal{L}_C \subset \text{Loc}_1(\Upsilon).$$

By the construction, it comes with an explicit defining system of equations, see Sections 2.1.3 & 2.1.4.

The non-commutative version of Lemma 1.22 is more complicated. We will discuss its explicit version elsewhere. It also follows from the general machinery developed in [BrD1], [BrD2].

1.3.6 The case when all surfaces S_i of the collection \mathcal{Q} are discs.

Filling all holes on the surface Σ_Q by discs, we get the compactified spectral surface $\Sigma_{\mathcal{T}}$.

If all surfaces of the diagram \mathcal{Q} are discs, the surface Υ_Q is the compactified spectral surface $\Sigma_{\mathcal{T}}$:

$$\Upsilon = \Sigma_{\mathcal{T}} \quad \text{if all surfaces } S_i \text{ of the collection } \mathcal{Q} \text{ are discs.} \tag{31}$$

This case is important for applications to character varieties. Denote by $\mathcal{U}_{[\mathcal{T}]} \subset \mathcal{X}_{[\mathcal{T}]}$ the substack of sheafs with trivial microlocalisation at the conormal bundles to strands of \mathcal{T} . Since any local system on a disc is trivial, $\text{Loc}_1(S_i)$ are points, and the image of the restriction map lands in $\mathcal{U}_{[\mathcal{T}]}$. So

$$\begin{aligned} \mathcal{L}_{\mathcal{Q}}^{\circ} &\subset \text{Loc}_1(\Sigma_{\mathcal{T}}). \\ \mathcal{L}_{[\mathcal{Q}]} &\subset \mathcal{U}_{[\mathcal{T}]}. \end{aligned} \tag{32}$$

Theorem 1.23. *Let \mathcal{Q} be a \mathcal{Q} -diagram of discs in a threefold inducing an alternating diagram \mathcal{T} on the boundary. Then $\mathcal{L}_{[\mathcal{Q}]} \subset \mathcal{U}_{[\mathcal{T}]}$ is a non-commutative cluster Lagrangian. Its cluster tori are symplectic tori $\text{Loc}_1(\Sigma_{\mathcal{T}})$ for the alternating diagrams \mathcal{T} in the same admissible deformation class.*

Theorem 1.23 follows immediately from Theorem 1.19. See Section 5.4.

1.3.7 Applications to (non-commutative) character varieties.

In Section 5 we describe a class of non-commutative cluster Lagrangians in the stack $\mathcal{U}_{m,S}$ parametrising m -dimensional R -local systems on a surface S with punctures, with unipotent monodromies around the punctures. Namely, we show that any threefold M bounding the surface S with the filled punctures gives rise to such non-commutative cluster Lagrangian $\mathcal{L}_m(M)$, and describe it by a system of equations.

The crucial step is done in Section 5.3, where we define a \mathcal{Q} -diagram of cooriented discs in M starting from a decomposition of M into tetrahedra, and an integer $m \geq 2$ - the rank of local systems on ∂M . Then we use Theorem 1.23. We describe the Lagrangian $\mathcal{L}_m(M)$ using the cluster \mathcal{A} -coordinates assigned in Section 5.2 to any \mathcal{Q} -diagram of cooriented discs in a threefold.

In the commutative setting the cluster K_2 -symplectic structure on the space $\mathcal{U}_{m,S}$ gives rise, via the Beilinson-Deligne *symbole modéré* [B], [D], to a canonical line bundle with connection on the cluster part of $\mathcal{U}_{m,S}$. Results of Section 5 provide a trivialization of its restriction to the Lagrangian $\mathcal{L}_m(M)$, depending on a choice of a \mathcal{Q} -diagram in M . This generalizes the work [DGG]. If $m = 2$, this is closely related to the work of Freed and Neitzke [FN].

1.3.8 Organization of the paper.

In Section 2.1 we describe the non-commutative Lagrangian for the basic \mathcal{Q} -diagram in the cube.

In Section 2.2 we prove one of the crucial results, Theorem 2.1.

In Section 2.3 we give another description of the basic non-commutative cluster Lagrangian. We relate it to the \mathcal{A} -coordinate description of the two by two move [GKo], uncovering the surprising A_4 -symmetry of the latter.

In Section 3 we introduce the boundary at infinity of a conical Lagrangian. It enters to the formulation of Theorem 1.19.

In Section 4 we construct spectral covers associated with a certain class (called ideal) of alternating and \mathcal{Q} -diagrams in threefolds. The construction uses zig-zag surfaces assigned to these diagrams.

In Section 5.1 we discuss non-commutative cluster \mathcal{A} -varieties and their canonical quotients, which carry a cluster symplectic structure, arising from \mathcal{Q} -diagrams in threefolds.

In Section 5.2 we show that a \mathcal{Q} -diagram of cooriented discs in a threefold M gives rise to a cluster Lagrangian in the cluster symplectic quotient of the \mathcal{A} -variety assigned to the boundary of M .

In Section 5.3 we define a \mathcal{Q} -diagram of cooriented discs in a threefold M starting from a decomposition of M into tetrahedra, and an integer $m \geq 2$ - the rank of local systems on ∂M .

In Section 5.4 we use all this to describe the non-commutative cluster Lagrangian $\mathcal{L}_m(M) \subset \mathcal{U}_{m,S}$.

Acknowledgment. The key result of the paper was obtained during the summer of 2021, when the first author held the Gretchen and Barry Mazur Chair at IHES. The paper was finished during his stay in IHES in 2025. The first author was partially supported by the NSF grant DMS-2153059. We are grateful to IHES and NSF for hospitality and support.

2 The basic non-commutative cluster Lagrangian

2.1 Non-commutative cluster Lagrangian for the basic \mathcal{Q} -diagram

2.1.1 The basic \mathcal{Q} -diagram.

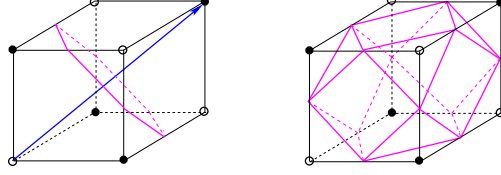


Figure 8: The central plane section perpendicular to a principal diagonal of the cube cuts a hexagon. The four planes cut a polyhedron with 8 triangular and 6 square faces. They cut the cube into four \circ -domains, four \bullet -domains, and six mixed domains. These domains are cones over the triangles assigned to the \circ/\bullet -vertices, and the squares.

Take a cube C as our threefold M . Its 1-skeleton is a bipartite ribbon graph Γ_{cube} , well defined up to switching $\bullet \leftrightarrow \circ$, see Figure 8. Consider the four planes H_1, \dots, H_4 passing through the center and perpendicular to the diagonals of the cube. We orient the diagonals by $\circ \rightarrow \bullet$. The planes are cooriented by the diagonals. The four planes form a \mathcal{Q} -diagram $\mathcal{Q}_{\text{cube}}$ with a single quadruple intersection point p . It is called the *basic \mathcal{Q} -diagram*. Each plane intersects the cube by a hexagon. These hexagons subdivide the cube into six squares and eight triangles. The hexagons can be deformed to a zig-zag loop γ_i on the graph Γ_{cube} , shown by arrows on the left of Figure 9. There are four zig-zag loops on Γ_{cube} , which match the \circ -vertices.

Pick a \bullet -vertex v . Denote by X_1, X_2, X_3 the monodromies around the faces sharing the vertex v , see Figure 9, understood as endomorphisms of the fiber L_v :

$$X_1, X_2, X_3 \in \text{End}(L_v). \quad (33)$$

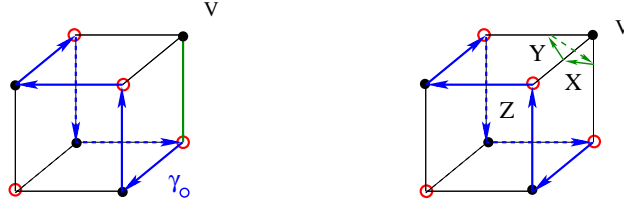


Figure 9: Let L_v be the fiber of a flat bundle L on the graph over a \bullet -vertex v . Then $X, Y, Z \in \text{End}(L_v)$ are monodromies around faces sharing v in the direction matching the cyclic order of the edges at v .

Denote by $\text{Loc}_1^{\text{tr}}(\Gamma_{\text{cube}})$ the substack of the non-commutative torus $\text{Loc}^{\text{tr}}(\Gamma_{\text{cube}})$ parametrising flat rank one bundles on the bipartite ribbon graph Γ_{cube} with trivial monodromy around zig-zag loops.

The following Theorem 2.1 is one of the main results of the paper. It is proved in Section 2.2.

Theorem 2.1. *For the basic \mathcal{Q} -diagram $\mathcal{Q}_{\text{cube}}$, the restriction functor (24) is a fully faithful embedding*

$$\text{Res}_{\partial C}^{\circ} : \mathcal{X}_{\mathcal{Q}_{\text{cube}}}^{\circ} \hookrightarrow \text{Loc}_1^{\text{tr}}(\Gamma_{\text{cube}}). \quad (34)$$

Its image $\mathcal{L}_{\mathcal{Q}_{\text{cube}}}^{\circ}$ is described by the following equations on monodromies $\{X_1, X_2, X_3\}$ in (33):

- For each \bullet -vertex v of the cube C we have:

$$X_1 X_2 X_3 + X_2 X_3 + X_3 = 0. \quad (35)$$

$$-X_1X_2X_3 = 1. \quad (36)$$

The equations (35) at the \bullet -vertices of the cube C are conjugate to each other, and thus are equivalent.

The monodromy Mon_γ along the zig-zag loop γ opposite to the \bullet -vertex v is given by:⁶

$$\text{Mon}_\gamma = -X_1X_2X_3. \quad (37)$$

The equation (36) just means that this monodromy is trivial.

Lemma 2.2. *The spectral surface for the bipartite surface graph Γ_{cube} is a torus T_4^* with four punctures. The group A_4 acts naturally on this torus. The completion T of the torus T_4^* is naturally isomorphic to the link of the Lagrangian \mathbb{L}_{cube} at the singular point. This isomorphism is A_4 -equivariant.*

Proof. It is a connected oriented surface homotopy equivalent to the graph Γ_{cube} . Its punctures match the zig-zag loops on the graph Γ_{cube} . So it must be a torus with four punctures. The group A_4 is realized as the group of symmetries of the cube preserving the bipartite graph.

The link of the Lagrangian \mathbb{L}_{cube} at the singular point is identified with the cone over the two dimensional Lagrangian associated with the zig-zag loops on the bipartite surface graph Γ_{cube} . \square

Let \mathcal{F} be an admissible sheaf inside of the cube C with the microlocal support at the Lagrangian \mathbb{L}_{cube} , which vanishes at the mixed domains. Then its restriction to the complement $C - q$ to the quadruple intersection point $q \in C$ is equivariant under dilations by the elements of R^\times . Therefore according to [GKo] it is described by a flat line bundle on the graph Γ_{cube} . Precisely, there is canonical equivalence between the category of such admissible sheaves in $C - q$ vanishing on the mixed domains, and the groupoid of flat line bundle on the graph Γ_{cube} . The latter groupoid is identified by Lemma 2.2 with the groupoid of flat line bundles on the punctured torus T_4^* . As we prove in Section 2.2, the condition that the intersection of the microlocal support of \mathcal{F} with T_p^*C is supported on the union of the conormals to the planes H_1, \dots, H_4 is equivalent to the equations (35)-(36) for all \bullet -vertices of Γ_{cube} . In particular the flat line bundle on the torus T_4^* assigned to \mathcal{F} extends to the punctures. Indeed, condition (36) just means that its monodromy around each of the punctures is trivial. Then the most interesting condition (35) specifies a Lagrangian in $\text{Loc}_1(T)$.

An important alternative description of this non-commutative Lagrangian is discussed in Section 2.3.

2.1.2 The K_2 -Lagrangian for commutative R .

The moduli space of flat line bundles on the graph Γ_{cube} is 5-dimensional: the cube has 6 faces, but the product of all face coordinates is equal to 1. The subvariety parametrising flat line bundles with trivial monodromies around zig-zag loops can be described by imposing the four monomial equations (36) assigned to the \bullet -vertices of the cube. The product of relations (36) over all \bullet -vertices is equal to 1. The resulting space is a two dimensional symplectic torus. It can be realized as the subtorus in the torus $(\mathbb{C}^\times)^3$ with coordinates X_1, X_2, X_3 , subject to the relation $X_1X_2X_3 = -1$. Then the symplectic form is $d \log(X_2) \wedge d \log(X_3)$. Its subspace $\mathcal{L}_{\mathbb{Q}_{\text{cube}}}^\circ$ is one dimensional, and hence automatically Lagrangian. However it is in fact K_2 -Lagrangian, which is a much stronger condition. It amounts to the fact that the equation $X_2X_3 + X_3 = 1$ implies that⁷

$$\{X_2, X_3\} = -\{X_2, 1 + X_2\} = 0 \quad \text{in } K_2 \text{ mod 2-torsion.}$$

2.1.3 Describing the stack $\mathcal{X}_{\mathbb{Q}}^\circ$.

Given any \mathbb{Q} -diagram \mathcal{Q} in a threefold M , let

$$\begin{aligned} M_\times &= M - \{\text{small open balls in } M \text{ around the quadruple intersection points}\}. \\ \mathcal{Q}_\times &:= \mathcal{Q} \cap M_\times. \end{aligned} \quad (38)$$

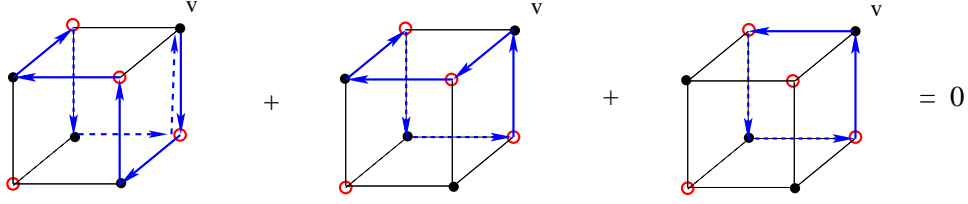


Figure 10: The relation $X_1X_2X_3 + X_2X_3 + X_3 = 0$. Together with the condition $X_1X_2X_3 = -1$, it reads $X_2X_3 + X_3 = 1$. Here X_i are the monodromies around the faces starting at the vertex v , as on Figure 9.

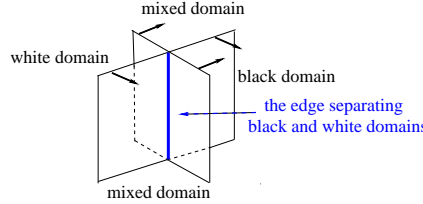


Figure 11: Intersection of two cooriented planes, and the edge separating the black and white domains.

Definition 2.3. Given a \mathcal{Q} -diagram $\mathcal{Q} \subset M$, we define a bipartite graph $\Gamma_{\mathcal{Q}}$. Its black (respectively white) vertices are the \bullet -domains (respectively the \circ -domains) of \mathcal{Q} . The edges between the vertices \mathcal{D}_{\bullet} and \mathcal{D}_{\circ} correspond to the edges of \mathcal{Q} separating the two domains, see Figure 11.

The edges of the graph $\Gamma_{\mathcal{Q}}$ which are incident to the vertex assigned to a colored polyhedron \mathcal{D} match the edges of the polyhedron.

Theorem 2.4. The stack $\mathcal{X}_{\mathcal{Q}_{\times}}^{\circ}$ is equivalent to the stack of rank one local systems on the graph $\Gamma_{\mathcal{Q}}$.

Proof. The stack $\mathcal{X}_{\mathcal{Q}_{\times}}^{\circ}$ is described the same way as for alternating diagrams on surfaces in [GKo]. \square

So since $\pi_1(\Gamma_{\mathcal{Q}})$ is a free group, the stack $\mathcal{X}_{\mathcal{Q}_{\times}}$ is a non-commutative torus.

Let

$$\mathbb{L}_{\times} := \mathbb{L} - \{\text{small open balls in } T^*M \text{ around the singular points of } \mathbb{L}\}. \quad (39)$$

Let q be a quadruple intersection point of \mathcal{Q} , and S_q^2 a little sphere around q . Then $\mathcal{Q}_{\times} \cap S_q^2$ is an alternating diagram on the sphere S_q^2 . The related bipartite surface graph is isomorphic to Γ_{cube} . The restriction to S_q^2 of any $\mathcal{F} \in \mathcal{X}_{\mathcal{Q}}^{\circ}$ is described by a flat line bundle $L_{\mathcal{F}}$ on the graph Γ_{cube} for which equations (35) from Theorem 2.1 hold.

The boundary of the Lagrangian \mathbb{L}_{\times} is the disjoint union of the surface Υ in (21), realised as the zero section in $T^*\Upsilon$, and the tori T_q given by the links of the singular points q of \mathbb{L} :

$$\partial\mathbb{L}_{\times} = \Upsilon \cup \bigcup_{q \in \text{Sing}(\mathbb{L})} T_q. \quad (40)$$

By Lemma 2.2, the torus T_q is the spectral surface of the bipartite surface graph Γ_{cube} , with filled punctures. So the space $\text{Loc}_1(T_q)$ carries a natural symplectic structure.

Therefore the functor of the restriction to the boundary Lagrangian $\partial\mathbb{L}_{\times}$ provides a Lagrangian

$$\Lambda_{\mathcal{Q}} := \text{Res}_{\partial\mathbb{L}_{\times}}(\mathcal{X}_{\mathcal{Q}_{\times}}^{\circ}) \subset \text{Loc}_1(\Upsilon) \times \prod_{q \in \text{Sing}(\mathbb{L})} \text{Loc}_1(T_q). \quad (41)$$

We view it as a Lagrangian correspondence. So it acts on the product of basic Lagrangians in $\text{Loc}_1(T_q)$, and the image of this action is the Lagrangian $\mathcal{L}_{\mathcal{Q}}$. Let us elaborate this.

⁶The $-$ sign reflects the fact that we work with twisted sheaves.

⁷Recall that the Steinberg relation $\{x, 1-x\}$ in K_2 implies that $\{z, -z\} = 0$, but $\{z, -1\}$ is only a 2-torsion.

2.1.4 Describing the Lagrangian $\mathcal{L}_{\mathcal{Q}}$ by equations.

Given symplectic manifolds $\mathcal{S}_1, \mathcal{S}_2$ and Lagrangians $L_1 \subset \mathcal{S}_1$ and $\mathcal{L} \subset \mathcal{S}_1 \times \mathcal{S}_2$, we get a Lagrangian $L_2 \subset \mathcal{S}_2$ by acting by the Lagrangian correspondence \mathcal{L} on the Lagrangian L_1 in the Weinstein category of symplectic spaces:

$$L_2 := \mathcal{L} \circ L_1 \subset \mathcal{S}_2.$$

We apply this to Lagrangian correspondence $\Lambda_{\mathcal{Q}}$ in (41). It acts on the product of basic Lagrangians

$$\prod_{q \in \text{Sing}(\mathbb{L})} \mathcal{L}_{\text{cube}} \subset \prod_{q \in \text{Sing}(\mathbb{L})} \text{Loc}_1(\mathbb{T}_q)$$

parametrised by the singular points q of the \mathcal{Q} -diagram \mathcal{Q} , and provides a Lagrangian in $\text{Loc}_1(\Upsilon_{\mathcal{Q}})$:

$$\Lambda_{\mathcal{Q}} \circ \prod_{q \in \text{Sing}(\mathbb{L})} \mathcal{L}_{\text{cube}} \subset \text{Loc}_1(\Upsilon_{\mathcal{Q}}). \quad (42)$$

It is described by the equations (35)-(36) parametrised by the singular points of \mathbb{L} . The resulting Lagrangian can be obtained explicitly by the elimination of variables.

2.2 Proof of Theorem 2.1

2.2.1 Set-up.

Let \mathcal{F} be an admissible sheaf on a threefold M , with the microlocal support at a \mathcal{Q} -diagram \mathcal{Q} , which vanishes on mixed domains. We give an explicit description of \mathcal{F} in that case. Assuming that \mathcal{F} is of microlocal rank one, we get a cluster description of the corresponding moduli space, as a subvariety in a non-commutative torus defined by the equations (35)-(36). This completes the proof of Theorem 2.1.

Let us first describe \mathcal{F} on the complement to quadruple intersection points. In this case the description is reduced to the 2d picture studied in [GKo, Section 10.1]. The restriction of \mathcal{F} to the interior of a \bullet -domain D_{\bullet} is a constant sheaf $V_{D_{\bullet}}$ in the degree 0. The restriction of \mathcal{F} to the interior of a \circ -domain D_{\circ} is the constant sheaf $V_{D_{\circ}}[-1]$ in the degree 1. Near an intersection of two surfaces from \mathcal{Q} , its transversal section is described on Figure 12.

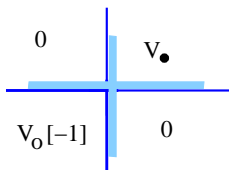


Figure 12: An admissible sheaf on a surface near an intersection point, vanishing on mixed domains, with the microlocal support at the shaded areas and at zero sections over quadrangles I & III. The fibers at punctured axes vanish. Objects V, W are in the degree 0. The structure map $h : V_{\circ}[-1] \rightarrow V_{\bullet}[-1]$ is an isomorphism.

Let us investigate now \mathcal{F} near a quadruple intersection point q . Denote by B a small ball around q . The restriction of \mathcal{F} to the punctured ball $B - q$ is determined by its restriction to the sphere ∂B . The latter is an admissible dg-sheaf \mathcal{F}_C with the microlocal support at zig-zag strands of the induced bipartite ribbon graph, identified with the graph Γ_C on the cube C . Here we use a natural topological identification $\partial B = C$. The dg-sheaf \mathcal{F}_C vanishes on mixed domains. The moduli space of such rank one admissible dg-sheaves for any bipartite ribbon graph is a non-commutative Poisson torus [GKo].

The restriction of the microlocal support of \mathcal{F} to $T_q^*M - \{0\}$ is a conical sheaf. Our condition on \mathcal{F} near the point q is this:

- The restriction of microlocal support of \mathcal{F} to $T_q^*M - \{0\}$ is concentrated on the four directed conormals η_1, \dots, η_4 to the cooriented surfaces of \mathcal{Q} intersecting at the quadruple intersection point q .

The fiber $\text{ml}(\mathcal{F})_\eta$ of the microlocal support of \mathcal{F} at a non-zero covector $\eta \in T_q^*M$ is described as follows. Take a small ball \mathcal{U} containing q . Denote by \mathcal{U}_η its little shift in the direction η . Then

$$\text{ml}(\mathcal{F})_\eta := \text{Cone}\left(\mathcal{F}_\mathcal{U} \xrightarrow{\text{res}} \mathcal{F}_{\mathcal{U} \cap \mathcal{U}_\eta}\right).$$

A priori we do not know the fiber $\mathcal{F}_q = \mathcal{F}_\mathcal{U}$. However by the condition •, the cone vanishes for any η other than the conormals to cooriented surfaces intersecting at q . So complexes $\mathcal{F}_{\mathcal{U} \cap \mathcal{U}_\eta}$, due to the isomorphism with \mathcal{F}_q , form a trivial local system on the punctured conormal sphere

$$S_q^2 - \{\eta_1, \dots, \eta_4\}, \quad S_q^2 := (T_q^*M - \{0\})/\mathbb{R}_{>0}.$$

Let us calculate the local system \mathcal{L} on $S_q^2 - \{\eta_1, \dots, \eta_4\}$ whose fiber at a covector η is given by

$$\mathcal{L}_\eta := \text{R}\Gamma(\mathcal{F}_{\mathcal{U} \cap \mathcal{U}_\eta}). \quad (43)$$

Then we impose the condition that the local system \mathcal{L} is trivial, and define \mathcal{F}_q as its fiber at generic η :

$$\mathcal{F}_q := \mathcal{L}_\eta. \quad (44)$$

Then there is a unique df-sheaf \mathcal{F} , whose restriction to $B - q$ was described above, and the fiber at q given by (44). Let us implement this plan.

From now on we identify topologically the conormal sphere S_q^2 and the cube C with the bipartite graph Γ_C . The covectors η_i point to the \circ -vertices of the cube, see Figure 8. We need to calculate the monodromy of the local system \mathcal{L} when the covector η goes around a cube \circ -vertex.

Pictures below depict zig-zag strands for the graph Γ_C , drawn on a relevant part of the cube surface.

2.2.2 Warm up: the local system around \bullet -vertex is trivial.

Consider the local system \mathcal{L} near a \bullet -vertex v_\bullet of the cube C on the ray spanned by the covector $-\eta_1$. The seven colored triangles on Figure 13 are intersections of triangular cones centered at q , containing all vertices of the cube except v_\bullet .

When the covector η is near $-\eta_1$, the spherical projection of the domain $\mathcal{U} \cap \mathcal{U}_\eta$ lies inside of a red disc - that is the disc inside of the red circle on Figure 13. The disc contains the central red triangle and one of the blue triangles. Triangles opposite to them do not intersect the disc. Other four triangles intersect the disc partially. The middle picture on Figure 13 tells that central triangle has sides cooriented inside of the triangle, by our convention on Figure 12. So it is a \bullet -triangle. The domain on the left of Figure 13 contains four red \bullet -triangles, three blue \circ -triangles, and three rectangles. There are six outside crossing points, depicted by \bullet on the left of Figure 13.⁸ The red disc contains three consecutive crossing points.

We claim that the local system \mathcal{L} near the covector $-\eta_1$ is trivial on the nose. Indeed, the domain $\mathcal{U} \cap \mathcal{U}_\eta$ for a covector η near $-\eta_1$ is the red disc on Figure 13. Let us calculate the parallel transport of the fiber \mathcal{L}_η of \mathcal{L} . Moving the η around the covector $-\eta_1$ amounts to moving the red disc around. There are six different positions of the disc, specified by the consecutive triples of the crossing points inside the disc. The first one is the red disc. The next is the green disc on the right of Figure 13, and so on.

Figures 12 - 13 tell that the fibers inside of the red triangles are $W_0, W_{12}, W_{23}, W_{31}$ in the degree 0, and inside the blue ones are $W_1[-1], W_2[-1], W_3[-1]$ in the degree 1. The fibers at the punctured arcs are zero. The fibers at the solid arcs are isomorphic to the fibers inside of the nearby blue triangle. For each crossing separating two colored domains there is an isomorphism between the objects at the domains:

$$W_i \xrightarrow{\sim} W_0, \quad i = 1, 2, 3; \quad W_j \xrightarrow{\sim} W_{ij}, \quad W_i \xrightarrow{\sim} W_{ij}, \quad i \neq j. \quad (45)$$

To calculate the complex $\text{R}\Gamma(\mathcal{F}_{\mathcal{U} \cap \mathcal{U}_\eta})$ we use the following general recipe:

⁸The only other crossing points are the three vertices of the red central triangle.

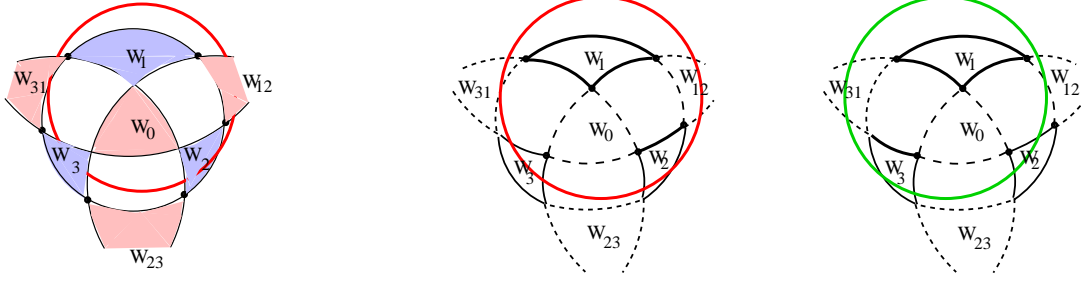


Figure 13: The local system \mathcal{L} is trivial on the nose.

- Given a domain \mathcal{U} intersecting strata by contractible subsets, to calculate $\mathrm{R}\Gamma\mathcal{F}_{\mathcal{U}}$ we restrict the data defining the dg-sheaf \mathcal{F} to \mathcal{U} . Then $\mathrm{R}\Gamma\mathcal{F}_{\mathcal{U}}$ is the complex provided by the restricted dg-sheaf data. We need only the restrictions to the strata \mathcal{V} which lie entirely in \mathcal{U} .

Therefore $\mathrm{R}\Gamma(\mathcal{F}_{\mathcal{U} \cap \mathcal{U}_\eta})$ for the red disc on Figure 13 is the following complex⁹ in degrees $[1, 2]$:

$$W_1 \oplus W_2 \oplus W_3 \longrightarrow W_0.$$

The similar complex for the green disc delivers the same result. Since the answer is invariant under the cyclic shift, the other four domains give the same. So the parallel transport from one domain to the other is trivial, and the local system \mathcal{L} is trivial, as expected, since \mathcal{F} has no microlocal support nearby $-\eta_1$.

2.2.3 The local system \mathcal{L} near a \circ -vertex.

Let us calculate the $\mathrm{R}\Gamma$ for the restriction of \mathcal{F} to the red disc on Figure 14. Figures 12 and 14 tell that the fibers at the points of blue domains are the objects $V_0[-1], V_{12}[-1], V_{23}[-1], V_{31}[-1]$ in the degree 1, and for the red ones are V_1, V_2, V_3 in the degree 0. For each crossing point there is an isomorphism between the objects at the colored domains:

$$\psi_{0,j} : V_0 \xrightarrow{\sim} V_j, \quad i = 1, 2, 3; \quad \varphi_{ij} : V_{ij} \xrightarrow{\sim} V_j, \quad \varphi_{ji} : V_{ij} \xrightarrow{\sim} V_i, \quad i \neq j. \quad (46)$$

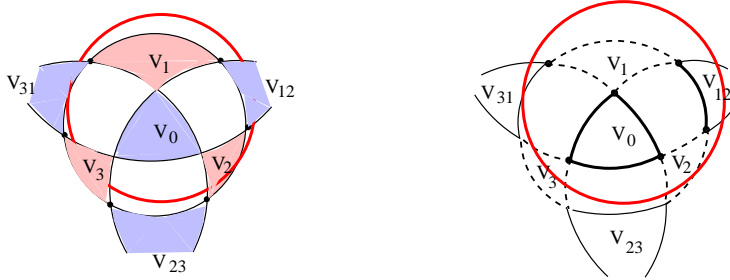


Figure 14: Calculating the $\mathrm{R}\Gamma$ for the restriction of a dg-sheaf \mathcal{F} to the red disc.

Let us introduce shorthands like:

$$V_{0+12+23} := V_0 \oplus V_{12} \oplus V_{23}, \quad V_{0+23+31} := V_0 \oplus V_{23} \oplus V_{31}, \quad V_{0+31+12} := V_0 \oplus V_{31} \oplus V_{12}, \quad \text{etc.}$$

⁹The central open triangle carries the object W_0 in the degree 0. The sheaf on the closed triangle is $j_!W_0$, where j is the embedding of the open triangle to the closed one. So we get the cohomology $W_0[-2]$. Equivalently, for a Čech cover of the triangle by open discs $\mathcal{U}_1, \mathcal{U}_2, \mathcal{U}_3$ centered at the vertices, only the section over $\mathcal{U}_1 \cap \mathcal{U}_2 \cap \mathcal{U}_3$ contributes, so we get $W_0[-2]$.

The recipe \bullet to the dg-sheaf for the red disc \mathcal{U} on Figure 14 gives the following complex in degrees $[1, 2]$:

$$V_{0+12+31} \rightarrow V_1. \quad (47)$$

Indeed, the domain with the object V_3 does not contribute. The punctured arc on the boundary of the domain V_2 , which lies inside of the red disc, contributes 0. The unique punctured triangle inside of the red disc contributes $V_0[-2]$. The blue triangles contribute $V_{31}[-1]$ and $V_{12}[-1]$: the first is the section over the vertex, and the second over the unique segment inside of the red disc.

There are quasiisomorphisms given by the quotients by acyclic subcomplexes $V_{13} \rightarrow V_1$ and $V_{12} \rightarrow V_1$:

$$\begin{aligned} (V_{0+12+13} \rightarrow V_1) &\rightarrow V_{0+12}. \\ (V_{0+12+13} \rightarrow V_1) &\rightarrow V_{0+13}. \end{aligned} \quad (48)$$

Rotating the red disc, so that it contains the next triple of crossings, we get the green disc on Figure 15.

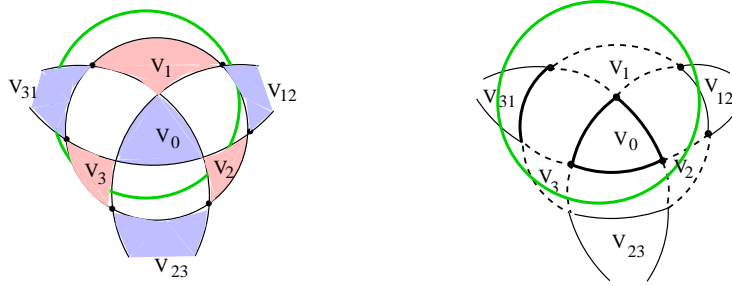


Figure 15: $R\Gamma(\mathcal{F})$ for the green disc is identified on the nose with $R\Gamma(\mathcal{F})$ for the red disc on Figure 14.

It produces the same on the nose complex (47). So the rotation amounts to the tautological isomorphism.

Rotating similarly the green disc we get the blue disc on Figure 16, and the complex degrees $[1, 2]$:

$$V_{0+31+23} \rightarrow V_3. \quad (49)$$

There are quasiisomorphisms given by the quotients by acyclic subcomplexes $V_{13} \rightarrow V_3$ and $V_{23} \rightarrow V_3$:

$$\begin{aligned} (V_{0+23+13} \rightarrow V_3) &\rightarrow V_{0+23}. \\ (V_{0+23+13} \rightarrow V_3) &\rightarrow V_{0+13}. \end{aligned} \quad (50)$$

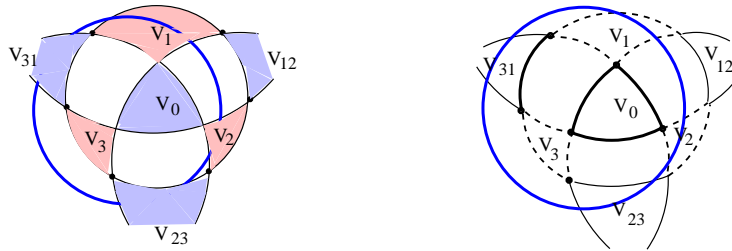


Figure 16: Calculating $R\Gamma(\mathcal{F})$ for the restriction of a dg-sheaf \mathcal{F} to the blue disc.

We repeat the disc rotations till we come back to the red disc on Figure 14. Then we get a diagram

of quasiisomorphisms:

$$\begin{array}{ccccc}
 & V_{0+12+23} \rightarrow V_2 & & V_{0+23+31} \rightarrow V_3 & & & & V_{0+31+12} \rightarrow V_1 & & \\
 & \swarrow & & \swarrow & & & & \swarrow & & \\
 V_{0+12} & & & V_{0+23} & & & & V_{0+31} & & V_{0+12}
 \end{array} \tag{51}$$

Let us calculate the composition of the quasiisomorphisms between the bottom objects in (51):

$$V_0 \oplus V_{12} \longrightarrow V_0 \oplus V_{23} \longrightarrow V_0 \oplus V_{31} \longrightarrow V_0 \oplus V_{12}. \tag{52}$$

Each of the maps in (52) is given by the 2×2 lower triangular matrix. Let us calculate their product.

1. The map $V_0 \longrightarrow V_0$ is the identity map since it is the composition of the identical maps:

$$V_0 \longrightarrow V_0 \longrightarrow V_0 \longrightarrow V_0.$$

2. The map $V_{12} \longrightarrow V_{12}$ amounts to the composition of the maps

$$V_{12} \longrightarrow V_{23} \longrightarrow V_{31} \longrightarrow V_{12}.$$

The latter is the composition of the six isomorphisms $V_{ij} \longrightarrow V_i$ and their inverces in (46):

$$V_{12} \longleftarrow V_2 \longrightarrow V_{23} \longleftarrow V_3 \longrightarrow V_{31} \longleftarrow V_1 \longrightarrow V_{12}. \tag{53}$$

3. The map $V_0 \longrightarrow V_{12}$ is given by the sum of the following three terms, defined below:

$$(55) + (56) + (57). \tag{54}$$

Each of them is obtained by composing the following "up and down" quasiisomorphisms:

$$\begin{array}{ccccccc}
 & & V_2 & & V_3 & & V_1 & & \\
 & & \swarrow & & \swarrow & & \swarrow & & \\
 V_0 & & & & V_{23} & & & & V_{12} \\
 & & \searrow & & \searrow & & \searrow & & \\
 & & & & & & & &
 \end{array} \tag{55}$$

$$\begin{array}{ccccccc}
 & & V_3 & & V_1 & & \\
 & & \swarrow & & \swarrow & & \\
 V_0 & & & & V_{31} & & V_{12} \\
 & & \searrow & & \searrow & & \\
 & & & & & &
 \end{array} \tag{56}$$

$$\begin{array}{ccc}
 & V_1 & \\
 & \swarrow & \searrow \\
 V_0 & & V_{12}
 \end{array} \tag{57}$$

Let us elaborate the isomorphism $V_0 \longrightarrow V_{23}$ from the left triangle in (55).

$$\begin{array}{ccc}
 & V_{0+12+23} \longrightarrow V_2 & \\
 & \swarrow & \searrow \\
 V_{0+12} & & V_0 \oplus V_{23}
 \end{array} \tag{58}$$

Let $(a, b) \in V_{0+12}$. It lifts to a cycle $(a, b, b') \rightarrow 0$ in the complex $V_{0+12+23} \longrightarrow V_2$, where $\psi_{0,2}(a) + \varphi_{12}(b) + \varphi_{32}(b') = 0$. Then it projects to the element

$$b' = -(\varphi_{32}^{-1} \circ \psi_{0,2}(a) + \varphi_{32}^{-1} \circ \varphi_{12}(b)) \in V_{23}.$$

We stress the $-$ sign in this formula by the sign $-$ in (55) - (57).

2.2.4 The meaning of conditions 2) and 3).

An admissible dg-sheaf near a quadruple intersection point which vanishes on mixed domains induces a similar dg-sheaf on the surface of the cube C . Since the latter vanishes on mixed domains, it is described by a rank one local system \mathcal{L}_C on the graph Γ_C .

White vertices w of the graph Γ_C match oriented diagonals bw of the cube, and hence the conormals $\eta_w \in \{\eta_1, \dots, \eta_4\}$, and the zig-zag loops on Γ_C . We denote by γ_w the zig-zag loop corresponding to w .

The composition (53) is the monodromy of \mathcal{L}_C along the zig-zag loop γ_{w_0} on Γ_C , see Figure 17.

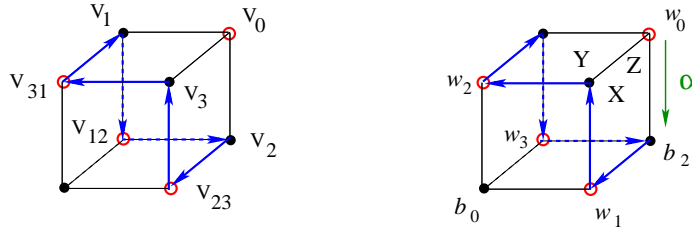


Figure 17: The zig-zag loop γ_{w_0} on the bipartite graph Γ_C . The monodromies $X_{w_0}, Y_{w_0}, Z_{w_0}$ along the loops based at the vertex w_0 , around the faces sharing w_0 . The faces are ordered clockwise.

Denote by X_w, Y_w, Z_w the monodromies around the faces sharing a \circ -vertex w , over the loops based at w . The order of the faces and the loop orientations are compatible with the cyclic order induced by the ribbon structure of Γ_C . It is the clockwise order on Figure 17, looking at the cube from the outside.

Denote by $\alpha_2\alpha_1$ the composition of a path α_1 followed by α_2 . Let α be the edge path $w_0 \rightarrow b_2$ on Figure 17. Then the monodromy Mon_{γ, b_2} along the zig-zag loop γ starting at the vertex b_2 is:

$$\alpha^{-1}\text{Mon}_{\gamma, b_2}\alpha = Z_{w_0}Y_{w_0}X_{w_0}. \quad (59)$$

There are obvious equalities, where on the right stands a map $V_0 \rightarrow V_0$ given by the composition:

$$\begin{aligned} - X_{w_0} &= V_0 \rightarrow V_2 \rightarrow V_{23} \rightarrow V_3 \rightarrow V_0, \\ - Y_{w_0} &= V_0 \rightarrow V_3 \rightarrow V_{31} \rightarrow V_1 \rightarrow V_0, \\ - Z_{w_0} &= V_0 \rightarrow V_1 \rightarrow V_{12} \rightarrow V_2 \rightarrow V_0. \end{aligned} \quad (60)$$

The $-$ sign on the left appears since we consider *twisted* dg-sheaves. So making a circle, we rotate the tangent vector by 2π , thus getting an extra -1 factor, while on the right stands the plain monodromy.

Lemma 2.5. *For each white vertex w of the graph Γ_C , the condition that composition (53) is the identity map for the conormal η_w just means that the local system \mathcal{L}_C on the graph Γ_C has trivial monodromy along the zig-zag loop γ_w . Equivalently, we have the monomial relation*

$$Z_w Y_w X_w = -1. \quad (61)$$

It is equivalent to the monomial relation (67).

Proof. The first and second claims follows from (59) and (60). The last claim ... \square

Lemma 2.6. *For each white vertex w of the bipartite graph Γ_C , the condition that the sum (54) is zero for the conormal η_w is equivalent to the following relation:*

$$Z_w Y_w + Z_w = 1. \quad (62)$$

Proof. Composing each of the maps (55) - (57) with the map $V_{12} \rightarrow V_0$ we get (62) by (60) and (61). \square

2.2.5 Conclusion.

Let q be a quadruple intersection point. Let \mathcal{F}° be an admissible dg-sheaf on the punctured ball $B - q$ vanishing on mixed domains. Then the condition that the composition (52) is the identity map is equivalent to the following two:

- (i) There is an admissible dg-sheaf \mathcal{F} on U whose restriction to $U - q$ is given by \mathcal{F}° , and
- (ii) The microlocal support of \mathcal{F} at q is supported at the conormals to surfaces of \mathcal{Q} intersecting at q .

2.3 The basic non-commutative cluster Lagrangian in \mathcal{A} -coordinates

In Section 2.3 we give an alternative description of the basic non-commutative cluster Lagrangian. It is in fact a description using the non-commutative \mathcal{A} -coordinates introduced in [GKo] and reviewed in Section 6.1. However Section 2.3 is essentially self-contained, and does not require the reader to know the definition of non-commutative \mathcal{A} -coordinates. In fact it provides the crucial example of the latter.

The description of the basic non-commutative cluster Lagrangian in Section 2.3 relates it to the non-commutative two by two move in \mathcal{A} -coordinates introduced in [GKo], and uncovers its surprising A_4 -symmetry.

2.3.1 An A_4 -invariant Lagrangian subvariety \mathbb{L} in a non-commutative torus $\mathcal{A}_{\text{cube}}$.

The 1-skeleton of the cube C is a bipartite graph Γ_{cube} , see Figure 18. It provides a non-commutative torus $\mathcal{A}_{\text{cube}}$, with the algebra of functions generated by the variables (a_i, b_i, c_i) , $i \in \mathbb{Z}/4\mathbb{Z}$, subject to the monomial relations, corresponding to the vertices of the cube:

$$\begin{aligned} a_4 a_1 c_1 = -1, \quad b_2 b_1 c_2 = -1, \quad a_2 a_3 c_3 = -1, \quad b_4 b_3 c_4 = -1; \\ b_1 b_4 c_1 = -1, \quad a_1 a_2 c_2 = -1, \quad b_3 b_2 c_3 = -1, \quad a_3 a_4 c_4 = -1. \end{aligned} \tag{63}$$

Here the first four relations are assigned to the \circ -vertices, and the last four to the \bullet -vertices.

Each monomial is the product of the variables at the edges sharing a vertex, in the order compatible with the cyclic order at the vertex, shown as counterclockwise on the pictures.

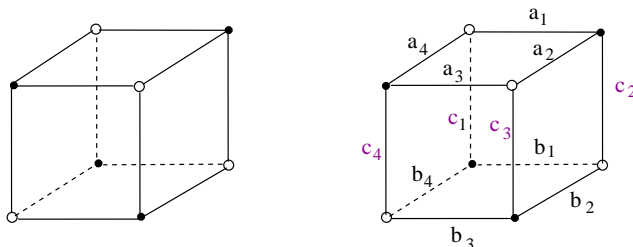


Figure 18: The bipartite ribbon graph Γ_{cube} on the cube. On the right: the \mathcal{A} -coordinates on the graph.

Recall the system (64) of 12 equations, illustrated on Figure 20:

$$\begin{aligned} a_4 b_2 + (c_3 c_1)^{-1} = 1, \quad b_2 a_4 + (c_4 c_2)^{-1} = 1, \\ a_2 b_4 + (c_1 c_3)^{-1} = 1, \quad b_4 a_2 + (c_2 c_4)^{-1} = 1, \\ \\ a_1 b_3 + (b_2 a_4)^{-1} = 1, \quad b_3 a_1 + (a_2 b_4)^{-1} = 1, \\ a_3 b_1 + (b_4 a_2)^{-1} = 1, \quad b_1 a_3 + (a_4 b_2)^{-1} = 1, \\ \\ c_1 c_3 + (b_3 a_1)^{-1} = 1, \quad c_3 c_1 + (b_1 a_3)^{-1} = 1, \\ c_2 c_4 + (a_3 b_1)^{-1} = 1, \quad c_4 c_2 + (a_1 b_3)^{-1} = 1. \end{aligned} \tag{64}$$

Theorem 2.7. Equations (64) define an A_4 -invariant Lagrangian subvariety \mathbb{L} in the non-commutative torus $\mathcal{A}_{\text{cube}}$ given by equations (63), with $a_i, b_i, c_i \in R^*$.

Theorem 2.7 is proved in Section 2.3.6.

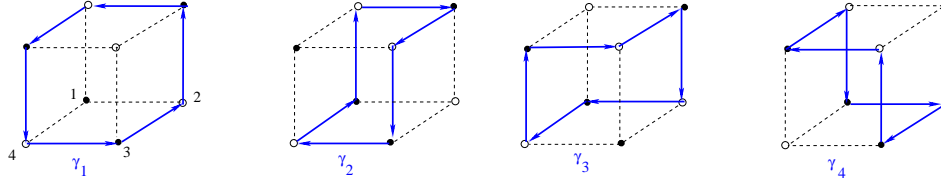


Figure 19: Four zig-zag hexagons $\gamma_1, \dots, \gamma_4$ on the cube.

We prove in Lemma 5.5 below that equations (63)+(64) are equivalent to the equations (36)+(35).

The system of equations (64) coincides with the one considered in [GKo, Section 6]. It was shown there that the latter describes the non-commutative cluster Lagrangian provided by the graph of the two by two move on non-commutative cluster \mathcal{A} -varieties, described by formulas (123). Our description makes evident the hidden A_4 -symmetry of this Lagrangian, which was totally obscure in (123).

Using monomial relations (63), equations (64) can be written in a polynomial form.¹⁰

$$\begin{aligned}
 a_4 b_2 + a_4 a_1 a_2 a_3 &= 1, & b_2 a_4 + a_1 a_2 a_3 a_4 &= 1. \\
 a_2 b_4 + a_2 a_3 a_4 a_1 &= 1, & b_4 a_2 + a_3 a_4 a_1 a_2 &= 1. \\
 a_1 b_3 + a_1 c_1 b_1 c_2 &= 1, & b_3 a_1 + c_1 b_1 c_2 a_1 &= 1. \\
 a_3 b_1 + c_2 a_1 c_1 b_1 &= 1, & b_1 a_3 + b_1 c_2 a_1 c_1 &= 1. \\
 c_1 c_3 + a_2 c_2 b_2 c_3 &= 1, & c_3 c_1 + c_3 a_2 c_2 b_2 &= 1. \\
 c_2 c_4 + c_2 b_2 c_3 a_2 &= 1, & c_4 c_2 + b_2 c_3 a_2 c_2 &= 1.
 \end{aligned} \tag{65}$$

2.3.2 Another perspective to equations (64).

There are four zig-zag hexagons on the bipartite graph Γ_{cube} on Figure 19. They correspond to the principal diagonals of the cube. Namely, the plane perpendicular to such a diagonal and passing through its center cuts a hexagon on the cube, which is the zig-zag loop assigned to this diagonal. Each zig-zag hexagon gives rise to three equations, described as follows. Zig-zags are oriented so that we turn right at \bullet -vertices, and turn left at \circ -vertices.¹¹ Pick a zig-zag γ , and a \bullet -vertex on it. Then the edges of γ are ordered starting at the edge exiting the \bullet -vertex and following the orientation of γ . Denote by $z_1, z_2, z_3, z_4, z_5, z_6$ the elements of R at the edges, see Figure 20.

Lemma 2.8. The elements $z_1, z_2, z_3, z_4, z_5, z_6 \in R^\times$ at the edges of γ satisfy the following equations:

$$z_1 z_4 + (z_5 z_2)^{-1} = 1, \quad z_5 z_2 + (z_3 z_6)^{-1} = 1, \quad z_3 z_6 + (z_1 z_4)^{-1} = 1. \tag{66}$$

$$z_3 z_6 \cdot z_1 z_4 \cdot z_5 z_2 = -1. \tag{67}$$

The relations are invariant under the cyclic shift by 2, and so independent on the choice of a \bullet -vertex.

¹⁰For example, since by (63) we have $a_4 a_1 = -c_1^{-1}$ and $a_2 a_3 = -c_3^{-1}$, we get $c_1^{-1} c_3^{-1} = a_4 a_1 a_2 a_3$. So the equation $a_4 b_2 + (c_3 c_1)^{-1} = 1$ from (64) is equivalent to $a_4 b_2 + a_4 a_1 a_2 a_3 = 1$ from (65). Note that the signs in monomial equations (63) can be altered without breacking the above arguments.

¹¹On the pictures we look to a face from the outside of the cube.

Proof. For example, for the zig-zag γ on Figure 20, the equations (66) are

$$a_4b_2 + (c_3c_1)^{-1} = 1, \quad c_3c_1 + (b_1a_3)^{-1} = 1, \quad b_1a_3 + (a_4b_2)^{-1} = 1. \quad (68)$$

Using monomial relations (63), we have $c_1b_1a_3a_4b_2c_3 = (b_3c_4b_4)^{-1} = (-1)^{-1} = -1$. Equivalently, $b_1a_3a_4b_2c_3c_1 = -1$. This is equivalent to (67). \square



Figure 20: An oriented zig-zag hexagon on the cube.

Proposition 2.9. *The monomial equation (67) follows from the monomial equations (63) at p .*

The twelve equations (66) assigned to the point p and four surfaces H_i intersecting at p are equivalent.

Proof. The three equations (66) are equivalent thanks to the following observation.

Lemma 2.10. *Let us assume that $xyz = -1$. Then the following three equations are equivalent:*

$$x + y^{-1} = 1 \iff y + z^{-1} = 1 \iff z + x^{-1} = 1.$$

Proof. Multiplying the first from the right by y and using $xy = -z^{-1}$ we get the second. And so on. \square

By Lemma 2.10, any equation in (64) is equivalent to one of the first four:

$$\begin{aligned} a_4b_2 + (c_3c_1)^{-1} = 1, & \quad b_2a_4 + (c_4c_2)^{-1} = 1. \\ a_2b_4 + (c_1c_3)^{-1} = 1, & \quad b_4a_2 + (c_2c_4)^{-1} = 1. \end{aligned} \quad (69)$$

Lemma 2.11. *Each of the equations (69) is obtained by conjugation of one of them.*

Proof. Conjugating the first equation by b_2 we get the second equation. Conjugating the third equation by b_4 we get the fourth equation. Conjugating the first equation by c_3 we get the third equation. \square

The proof of Proposition 2.9 follows immediately from these lemmas. \square

2.3.3 The rescaling action.

Let us label principal diagonals of the cube by the set $\mathbb{Z}/4\mathbb{Z}$, so that the i -th diagonal contains the vertex sharing the edges with the coordinates a_{i-1}, a_i on Figure 20. Denote by γ_i the zig-zag hexagon perpendicular to the i -th diagonal. Then an edge E carries the zig-zag assigned to the diagonals generating the plane parallel to the edge E .

Let us rescale each section s_γ trivializing the line bundle on the zig-zag γ by $s_\gamma \mapsto \lambda_\gamma s_\gamma$.

Rescaling the sections s_{γ_i} by λ_i provides an action of the group $(R^\times)^4$ on the \mathcal{A} -coordinates:

$$\begin{aligned} a_1 &\mapsto \lambda_1^{-1} a_1 \lambda_2, & a_2 &\mapsto \lambda_2^{-1} a_2 \lambda_3, & a_3 &\mapsto \lambda_3^{-1} a_3 \lambda_4, & a_4 &\mapsto \lambda_4^{-1} a_4 \lambda_1, \\ b_1 &\mapsto \lambda_4^{-1} b_1 \lambda_3, & b_2 &\mapsto \lambda_1^{-1} b_2 \lambda_4, & b_3 &\mapsto \lambda_2^{-1} b_3 \lambda_1, & b_4 &\mapsto \lambda_3^{-1} b_4 \lambda_2, \\ c_1 &\mapsto \lambda_2^{-1} c_1 \lambda_4, & c_2 &\mapsto \lambda_3^{-1} c_2 \lambda_1, & c_3 &\mapsto \lambda_4^{-1} c_3 \lambda_2, & c_4 &\mapsto \lambda_1^{-1} c_4 \lambda_3. \end{aligned} \quad (70)$$

The diagonal subgroup R^\times acts by the conjugation.

Proposition 2.12. *The action (70) of the group $(R^\times)^4$ on \mathcal{A} -coordinates has the following properties:*

- i) *Conjugates equations (63) - (64).*
- ii) *Preserves the non-commutative 2-form Ω .*

Proof. i) The action of the group $(R^\times)^4$ conjugates monomial equations (63):

$$a_i a_{i+1} c_2 \mapsto \lambda_i^{-1}(a_i a_{i+1} c_2) \lambda_i; \quad b_{i+1} b_i c_{i+1} \mapsto \lambda_i^{-1}(b_{i+1} b_i c_{i+1}) \lambda_i, \quad \forall i \in \mathbb{Z}/4\mathbb{Z}.$$

Each monomial $z_a z_{a+3}$ in relation (66) assigned to a zig-zag γ_i is conjugated by λ_i^{-1} . So each of the three relations assigned to a zig-zag γ_i is conjugated by λ_i^{-1} , e.g.

$$a_4 b_2 + (c_3 c_1)^{-1} \mapsto \lambda_4^{-1}(a_4 b_2 + (c_3 c_1)^{-1}) \lambda_4.$$

ii) Set $\{a, b\}' := dadbb^{-1}a^{-1}$. We have

$$\{a_i, a_{i+1}\}' \mapsto \lambda_i^{-1}\{a_i, a_{i+1}\}' \lambda_i, \quad \{b_{i+1}, b_i\}' \mapsto \lambda_i^{-1}\{b_{i+1}, b_i\}' \lambda_i.$$

The 2-form $\{a, b\}$ is the projection of $\{a, b\}'$ to the coinvariants of the cyclic shift. \square

2.3.4 Comparing with mutation formulas for the \mathcal{A} -coordinates from [GKo].

One can rewrite equations (64), using monomial relations (63) to eliminate c_i 's, as a birational transformation:

$$(a_1, a_2, a_3, a_4) \mapsto (b_1, b_2, b_3, b_4), \quad (71)$$

$$\begin{aligned} a_4 b_2 &= 1 - a_4 a_1 a_2 a_3, & b_2 a_4 &= 1 - a_1 a_2 a_3 a_4, \\ a_2 b_4 &= 1 - a_2 a_3 a_4 a_1, & b_4 a_2 &= 1 - a_3 a_4 a_1 a_2. \end{aligned} \quad (72)$$

Monomial relations (63) imply $a_i a_{i+1} = b_{i+1} b_i$, $i \in \mathbb{Z}/4\mathbb{Z}$. However the A_4 -symmetry is broken.

On the other hand, formulas (123) for a two by two move, borrowed from [GKo], look as follows:

$$\begin{aligned} a_4 \bar{b}_2^{-1} &= 1 - a_4 a_1 a_2 a_3, & \bar{b}_2^{-1} a_4 &= 1 - a_1 a_2 a_3 a_4, \\ a_2 \bar{b}_4^{-1} &= 1 - a_2 a_3 a_4 a_1, & \bar{b}_4^{-1} a_2 &= 1 - a_3 a_4 a_1 a_2. \end{aligned} \quad (73)$$

Formulas (73) transform to formulas (72) via the substitution

$$\bar{b}_i := b_i^{-1}, \quad i \in \mathbb{Z}/4\mathbb{Z}.$$

Here is the explanation. A flip of a triangulation of the rectangle $ABCD$ does not change the rectangle orientation. On the other hand, let us cut a tetrahedron into two rectangles, see Figure 21. We can identify the rectangles matching the corresponding edges. However then their orientations inherited from an orientation of the tetrahedron are opposite to each other. Changing the orientation of a bipartite graph means changing the cyclic orders of the edges at vertices to the opposite one. The \mathcal{A} -coordinates on the edges change as follows:

$$a_E \longrightarrow \bar{a}_E := a_E^{-1}. \quad (74)$$

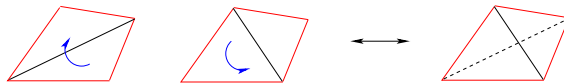


Figure 21: Cutting a tetrahedron into two rectangles induces the opposite orientations of rectangles.

Summarising, we get the following result.

Theorem 2.13. *Mutation formulas (72) for the non-commutative cluster \mathcal{A} -transformation corresponding to a two by two move are equivalent to the system of equations (64), where the variables (a_i, b_i, c_i) are related by monomial relations (63), corresponding to the cube vertices.*

2.3.5 Geometry of the two by two move.

Take a tetrahedron T . Consider the octahedron O given by the convex hull of the centers of the edges of T . Let C be the cube given by the convex hull of the centers of the faces of the octahedron O . It carries a graph Γ_C given by the 1-skeleton of the cube C . The graph Γ_C is a bipartite graph: its \bullet -vertices correspond to the triangles of the octahedra O which lie on the faces of the tetrahedra, see Figure 22.

The bipartite graph Γ_C on Figure 22 is identified with the one on Figure 18. The coordinates on the edges of Γ_C are identified with coordinates on the edges of the octahedra. We identify them with coordinates on the blue edges in the two by two move, see Figure 22. So there are bijections:

$$\{\text{green edges of the cube } C\} = \{\text{red edges of the octahedron } O\} = \{\text{blue edges of the two by two move}\}.$$

By the duality between the cube and the octahedron, the \mathcal{A} -variables are assigned to the edges of the

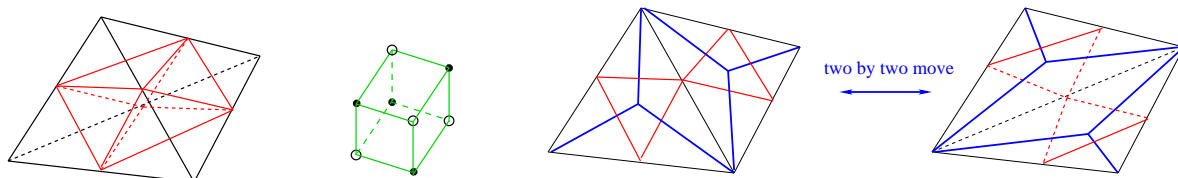


Figure 22: On the left: a black tetrahedron & the inscribed red octahedron. In the middle: the green cube, inscribed into the red octahedron, with a bipartite graph. On the right: a two by two move, blue.

octahedron O , and the monomial relations correspond to the triangular faces of the octahedron. Then the \mathcal{A} -variables are assigned to the edges of the blue cube, given by the union of the two blue graphs on the right of Figure 22. The blue cube has two kind of vertices: the centers of the faces of the tetrahedra, and the vertices of the tetrahedra. So we get the bipartite graph on the 1-skeleton of the cube.

2.3.6 Proof of Theorem 2.7.

We already know that \mathbb{L} is isotropic for the canonical 2-form Ω . On the other hand, take a generic quadruple $(\mathcal{A}, \mathcal{B}, \mathcal{C}, \mathcal{D})$ of decorated flags in a 2-dimensional R -vector space. Then a triangulation AC of the rectangle $ABCD$ gives rise to a collection of cluster \mathcal{A} -coordinates on the corresponding bipartite graph Γ_2 . A flip of this triangulation provides a collection of cluster \mathcal{A} -coordinates for the corresponding mutated bipartite graph Γ'_2 . Note that this is also a corollary of the very general claim in Theorem 5.4.

2.3.7 The commutative case.

The commutative torus $\mathcal{A}_{\text{cube}}$ is 5-dimensional. Indeed, there are 12 \mathcal{A} -variables at the edges of the cube. There are 8 monomial relations r_v assigned to the vertices v of the cube, see (63). There is a single relation between the relations:

$$\prod_{\bullet\text{-vertices } b} r_b = \prod_{\circ\text{-vertices } w} r_w.$$

So we get a torus of dimension $12 - 8 + 1 = 5$. It describes moduli space of 2-dimensional local systems on the 4-punctured sphere with a choice of an invariant vector near each puncture, considered modulo simultaneous rescaling of all of them.

The group $(R^\times)^4$ acts by rescaling of trivializations of the four zig-zags. The diagonal subgroup R_{diag} acts trivially. So we get a torus of dimension $12 - 8 + 1 - 3 = 2$.

3 Boundaries at infinity of singular Lagrangians

3.0.1 The Lagrangian $\mathbb{L}_{\mathcal{H}} \subset T^*X$.

Let X be a manifold with boundary Y , which carries a finite collection \mathcal{H} of smooth cooriented hypersurfaces $\{H_i\}$ with disjoint Legendrians. We assume that the hypersurfaces H_i intersect the boundary transversally by smooth cooriented hypersurfaces $\partial H_i \subset Y$ with disjoint Legendrians. Consider the Lagrangian in T^*X given by the zero section X° and the conormal bundles to the oriented hypersurfaces:

$$\mathbb{L} = \mathbb{L}_{\mathcal{H}} := X^\circ \cup \coprod_i T^*_{H_i} X. \tag{75}$$

3.0.2 The boundary Lagrangian $\partial(\mathbb{L}_{\mathcal{H}})$.

Our goal is define the boundary of the Lagrangian $\mathbb{L} = \mathbb{L}_{\mathcal{H}}$, which is a Lagrangian of the dimension one less in a symplectic space \mathcal{S} introduced below:

$$\partial\mathbb{L} \subset \mathcal{S}. \tag{76}$$

It is instructive to give the answer first in the case when the boundary Y is empty.

Take a sufficiently large compact $C \subset \mathbb{L}$, so that $\mathbb{L} - C$ is a union of components $\mathbb{R}_{[0,\infty)} \times H_i$:

$$\mathbb{L} - C = \coprod_i \left(\mathbb{R}_{[0,\infty)} \times H_i \right).$$

Let $H_{i,\infty}$ be the copy of H_i , perceived as $\infty \times H_i$. Then $\partial\mathbb{L}$ is the boundary at infinity $\partial_\infty\mathbb{L}$, defined as the zero section Lagrangian in the symplectic space $\mathcal{S} := \coprod T^*H_{i,\infty}$, see Figure 23:

$$\partial\mathbb{L} := \partial_\infty\mathbb{L} := \coprod H_{i,\infty} \subset \coprod T^*H_{i,\infty}. \tag{77}$$

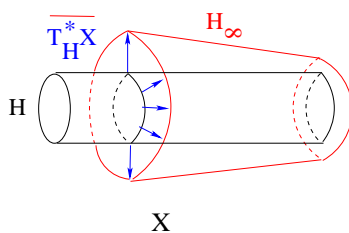


Figure 23: The hypersurface H_∞ is the boundary at infinity of $T^*_H X$. The Lagrangian $\partial_\infty\mathbb{L}$ is the zero section of T^*H_∞ .

Now let H be a single cooriented hypersurface in X with boundary $\partial H \subset Y$, and $L = T^*_H X$.

Let us define the following diagram:

$$\begin{array}{ccc}
 T^*Y & & T^*H \\
 \cup \alpha_2 \uparrow & & \cup \beta_2 \uparrow \\
 T^*_{\partial H} Y & & H \\
 \cup \alpha_1 \uparrow & & \cup \beta_1 \uparrow \\
 \partial H \times [0, 1] & \xrightarrow{=} & \partial H \times [0, 1]
 \end{array} \tag{78}$$

The map α_1 is the embedding of a collar neighborhood $\partial H \times [0, 1]$ of the zero section to $T_{\partial H}^* Y$. The map $\alpha_2 : T_{\partial H}^* Y \hookrightarrow T^* Y$ is the natural map. The map β_1 identifies $\partial H \times [0, 1]$ with a collar neighborhood of ∂H in H . The β_2 is the zero section $H \hookrightarrow T^* H$. Composing the vertical maps, we get the diagram

$$\begin{array}{ccc} T^* Y & & T^* H \\ & \swarrow \alpha_2 \circ \alpha_1 & \nearrow \beta_2 \circ \beta_1 \\ & \partial H \times [0, 1] & \end{array} \quad (79)$$

We define the symplectic variety \mathcal{S} by gluing symplectic varieties $T^* Y$ and $T^* H$ over $\partial H \times [0, 1]$, embedded to $T^* Y$ by the map $\alpha_2 \circ \alpha_1$, and to $T^* H$ by the map $\beta_2 \circ \beta_1$, see diagram (79):

$$\mathcal{S} := T^* Y *_{\partial H \times [0, 1]} T^* H. \quad (80)$$

The Lagrangian $\partial \mathbb{L}$ is obtained by a similar gluing, using the bottom half of diagram (78), see Figure 24:

$$\partial \mathbb{L} := \left(Y^\circ \cup T_{\partial H}^* Y \right) *_{\partial H \times [0, 1]} H. \quad (81)$$

The embedding $\partial \mathbb{L} \subset \mathcal{S}$ is induced from the embeddings $Y^\circ \cup T_{\partial H}^* Y \hookrightarrow T^* Y$ and $H \hookrightarrow T^* H$.

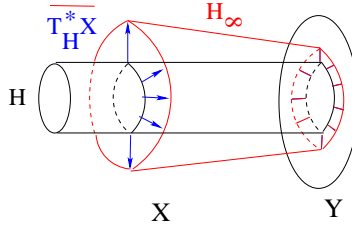


Figure 24: The Lagrangian $\partial \mathbb{L}$ is obtained by gluing the boundary end $\partial(H_\infty)$ of $\partial_\infty \mathbb{L} = H_\infty$ with the boundary at infinity $(\partial H)_\infty$ of $T_{\partial H}^* Y$.

Applying this construction to the union of hypersurfaces H_i we get the symplectic space \mathcal{S} and the Lagrangian $\mathbb{L} \subset \mathcal{S}$ in general.

Definition 3.1. *Given a finite collection of smooth hypersurfaces $\{H_i\}$ with disjoint Legendrians in a manifold X with the boundary Y , the symplectic variety \mathcal{S} is defined by gluing $T^* Y$ and $\coprod_i T^* H_i$:*

$$\mathcal{S} := T^* Y *_{\coprod_i \partial H_i \times [0, 1]} \coprod_i T^* H_i. \quad (82)$$

Its Lagrangian $\partial \mathbb{L}$ is defined by

$$\partial \mathbb{L} := \mathbb{L}_Y *_{\coprod_i \partial H_i \times [0, 1]} \coprod_i H_i, \quad (83)$$

where $\mathbb{L}_Y := Y^\circ \cup \cup_i T_{\partial H_i}^* Y \subset T^* Y$.

3.0.3 The boundary at infinity of Lagrangians.

Here is a more general picture. Let \mathbb{L} be a possibly singular non-compact closed Lagrangian subset in a symplectic space M , which contains a compact C , such that $\mathbb{L} - C$ has the following shape. There exists a possibly singular Lagrangian \mathbb{L}' of the dimension one less than \mathbb{L} in a symplectic space $U_\varepsilon(L')$, which can be retracted to \mathbb{L}' , and a neighborhood M_ε in M , such that

$$(\mathbb{L} - C \subset M_\varepsilon) = \left(\mathbb{L}' \subset U_\varepsilon(L') \right) \times \left([0, \infty) \subset ([0, \infty) \times (-\varepsilon, \varepsilon)) \right), \quad \dim(\mathbb{L}') = \dim(\mathbb{L}) - 1.$$

The second factor is the Lagrangian $[0, \infty)$ in a plane (p, q) , where $0 \leq p < \infty$ and $-\varepsilon < q < \varepsilon$, with the symplectic form $dp \wedge dq$, so that

$$\mathbb{L} - C = \mathbb{L}' \times [0, \infty).$$

Then the boundary at infinity $\partial_\infty \mathbb{L}$ is the Lagrangian \mathbb{L}' in the symplectic space $U_\varepsilon(\mathbb{L}')$:

$$\partial_\infty \mathbb{L} := \mathbb{L}' \subset U_\varepsilon(\mathbb{L}').$$

In particular, consider a smooth hypersurface H without the boundary in a manifold X . It gives rise to the Lagrangian \mathbb{L} given by the union of T_H^*X and the zero section X° . The Lagrangian \mathbb{L} has singularity at $T_H^*X \cap X^\circ$ of type (a single vertex graph with 3 edges) $\times \mathbb{R}^{n-2}$, where $n = \dim(X)$. Then applying the general definition above we arrive at the definition (77).

One can define Lagrangians at infinity with corners. Let us spell the case of codimension one corners, which is relevant to our story. In this case we assume that the complement $\mathbb{L} - C$ has two ends. Namely, there exists a possibly singular Lagrangian \mathbb{L}'' of the dimension two less than \mathbb{L} in a symplectic space $U_\varepsilon(\mathbb{L}'')$, which can be retracted to \mathbb{L}' , and a neighborhood M_ε in M , such that

$$\mathbb{L} - C = \left(\mathbb{L}'' \subset U_\varepsilon(\mathbb{L}'') \right) \times \left([0, \infty)^2 \subset ([0, \infty) \times (-\varepsilon, \varepsilon))^2 \right), \quad \dim(\mathbb{L}'') = \dim(\mathbb{L}) - 2.$$

The second factor is the subspace of the symplectic space \mathbb{R}^4 with coordinates (p_1, q_1, p_n, q_n) with the symplectic form $dp_1 \wedge dq_1 + dp_n \wedge dq_n$, given by $0 \leq p_n, q_1 < \infty$ and $-\varepsilon < q_n, p_1 < \varepsilon$. It contains the Lagrangian $[0, \infty)^2$ with coordinates (p_n, q_1) . We compactify it to a square $[0, \infty]^2$. The two sides of the square containing the corner (∞, ∞) form an angle $([0, \infty] \times \{\infty\}) \cup (\{\infty\} \times [0, \infty])$. The corner Lagrangian $\partial_{(2)} \mathbb{L}$ is the product of the Lagrangian \mathbb{L}'' and the angle:

$$\partial_{(2)}(\mathbb{L}) := \mathbb{L}'' \times \left(([0, \infty] \times \{\infty\}) \cup (\{\infty\} \times [0, \infty]) \right).$$

It contains the corner $\mathbb{L}'' \times \{\infty\}^2$. The Lagrangian $\partial_{(2)}(\mathbb{L})$ lies in the symplectic space

$$\partial_{(2)}\mathcal{S} = U_\varepsilon(\mathbb{L}'') \times \left(([0, \infty] \times \{\infty\}) \cup (\{\infty\} \times [0, \infty]) \right) \times (-\varepsilon, \varepsilon)^2.$$

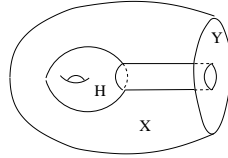


Figure 25:

3.0.4 The sheaf of categories $\mathcal{C}_{\mathbb{L}}$ and its restriction to the boundary Lagrangian.

Recall the singular Lagrangian \mathbb{L} in (75), and the sheaf of categories $\mathcal{C}_{\mathbb{L}}$ on \mathbb{L} , discussed in Section 1.3.1. Recall the zero section $H^\circ \subset T^*H$. For open sets $\mathbb{R}_{(a, \infty]} \times H_i$ there are canonical equivalences

$$\begin{aligned} \mathcal{C}_{\mathbb{R}_{(a, \infty]} \times H_i} &\xrightarrow{\sim} \mathcal{C}_{H_i}; \\ \mathcal{C}_{\mathbb{L} - C} &= \prod_i \mathcal{C}_{\mathbb{R}_{(a, \infty]} \times H_i} \xrightarrow{\sim} \prod_i \mathcal{C}_{H_{i, \infty}^\circ}. \end{aligned} \tag{84}$$

So the restriction functor $\text{Res}_{\mathbb{L} - C} : \mathcal{C}_{\mathbb{L}} \rightarrow \mathcal{C}_{\mathbb{L} - C}$ provides, using (84), the restriction at infinity functor

$$\text{Res}_\infty : \mathcal{C}_{\mathbb{L}} \rightarrow \mathcal{C}_{H_\infty^\circ} := \prod_i \mathcal{C}_{H_{i, \infty}^\circ}.$$

The transversal intersection of the collection of hypersurfaces \mathcal{H} with the boundary ∂X induces a collection $\partial\mathcal{H}$ on the boundary. There is the Lagrangian $\mathbb{L}_{\partial\mathcal{H}} \subset T^*\partial X$, see (75). The restriction to the boundary ∂X of X provides the functor

$$\text{Res}_{\partial X} : \mathcal{C}_{\mathbb{L}} \longrightarrow \mathcal{C}_{\mathbb{L}_{\partial\mathcal{H}}}.$$

There are also the restriction functors, where the bottom line functors are provided by the top line:

$$\begin{aligned} \mathcal{C}_{H_i^\circ} &\longrightarrow \mathcal{C}_{\partial H_i^\circ}, & \mathcal{C}_{\mathbb{L}_{\partial\mathcal{H}}} &\longrightarrow \mathcal{C}_{\partial H_i^\circ}. \\ \mathcal{C}_{\mathcal{H}_\infty} &\longrightarrow \mathcal{C}_{\partial\mathcal{H}_\infty}, & \mathcal{C}_{\mathbb{L}_{\partial\mathcal{H}}} &\longrightarrow \mathcal{C}_{\partial\mathcal{H}_\infty}. \end{aligned} \quad (85)$$

The functors Res_∞ and $\text{Res}_{\partial X}$ gives rise to the restriction functor to the fibered product of categories:

$$\text{Res} : \mathcal{C}_{\mathbb{L}} \longrightarrow \mathcal{C}_{\mathcal{H}_\infty} \times_{\mathcal{C}_{\partial\mathcal{H}_\infty}} \mathcal{C}_{\mathbb{L}_{\partial\mathcal{H}}}. \quad (86)$$

The following can be reduced from the results of Brav-Dyckerhoff [BrD1]-[BrD2].

Theorem 3.2. *The image of the restriction functor (86) is derived Lagrangian.*

3.0.5 The case of threefolds.

Consider a threefold M with boundary ∂M , equipped with a \mathcal{Q} -collection of smooth cooriented surfaces $\{S_i\}$. Recall the smooth closed surface $\Upsilon_{\mathcal{Q}}$.

Lemma 3.3. *The boundary $\partial\mathbb{L}^\circ$ of the Lagrangian \mathbb{L}° is the smooth closed surface $\Upsilon_{\mathcal{Q}}$:*

$$\partial\mathbb{L}^\circ = \Upsilon_{\mathcal{Q}}.$$

The restriction to the boundary provides projections

$$\begin{aligned} \pi_1 : \text{Loc}_1(\Sigma) &\longrightarrow \text{Loc}_1(\partial\Sigma). \\ \pi_2 : \text{Loc}_1(S_i) &\longrightarrow \text{Loc}_1(\partial S_i). \end{aligned} \quad (87)$$

Recall the restriction functor:

$$\text{Res}_{\partial\mathbb{L}^\circ} : \mathcal{C}_{\mathbb{L}}^\circ \longrightarrow \prod_i \text{Loc}_1(S_i) \times_{\text{Loc}_1(\partial\Sigma)} \mathcal{C}_{\mathcal{T}}^\circ. \quad (88)$$

The category $\mathcal{C}_{\mathcal{T}}^\circ$ is equivalent to the groupoid $\text{Loc}_1(\Sigma)$. So we arrive at the restriction functor

$$\text{Res}_{\partial\mathbb{L}^\circ} : \mathcal{C}_{\mathbb{L}}^\circ \longrightarrow \text{Loc}_1(\Upsilon_\Sigma) = \prod_i \text{Loc}_1(S_i) \times_{\text{Loc}_1(\partial\Sigma)} \text{Loc}_1(\Sigma). \quad (89)$$

Theorem 3.4. *The image of the restriction functor (89) is Lagrangian.*

In particular, if the surfaces S_i are discs, we get a Lagrangian subvariety

$$\text{Res}_{\partial\mathbb{L}^\circ}(\mathcal{C}_{\mathbb{L}}^\circ) \subset \text{Loc}_1(\Sigma). \quad (90)$$

Proof. The first claim follows from Theorem 3.2. If surfaces S_i are discs, then $\text{Loc}_1(S_i)$ are points, and the restriction functor (89) boils down to $\text{Res}_{\partial\mathbb{L}^\circ} : \mathcal{C}_{\mathbb{L}}^\circ \longrightarrow \text{Loc}_1(\Sigma)$. \square

4 Spectral covers for alternating and \mathcal{Q} -diagrams in threefolds

Let M be a threefold. Let \mathcal{Q} be a \mathcal{Q} -diagram in M . Recall the Lagrangian $\mathbb{L}_{\mathcal{Q}}^{\circ}$, and its subset $\mathbb{L}_{\times}^{\circ}$ obtained by cutting out singular points of $\mathbb{L}_{\mathcal{Q}}^{\circ}$, which correspond to quadruple intersection points of \mathcal{Q} . Recall the threefold

$$M_{\times} := M - \{\text{quadruple intersection points}\}.$$

In Section 4, under mild assumptions on \mathcal{Q} , we construct a smooth threefold with boundary $\Sigma_{\mathcal{Q}}$. The threefold $\Sigma_{\mathcal{Q}}$ is homeomorphic to $\mathbb{L}_{\times}^{\circ}$, and comes with a finite projection

$$\pi_{\mathcal{Q}} : \Sigma_{\mathcal{Q}} \longrightarrow M_{\times}.$$

To achieve this, we construct the spectral cover for an alternating diagram \mathcal{H} in M . The construction uses *zig-zag surfaces* assigned to alternating diagrams. We apply this construction to the alternating diagram obtained by resolving quadruple intersection points of \mathcal{Q} , and cutting out the obtained \bullet -tetrahedra.

4.0.1 A singular surface $\mathbb{S}_{\mathcal{H}}$ for an alternating diagram \mathcal{H} .

Let \mathcal{H} be an alternating diagram in a threefold M . Its singular points are the isolated triple intersection points, and the *edges* E , given by components of the singular locus of \mathcal{H} minus triple intersection points.

Let us assume that the \bullet - and \circ -domains are polyhedrons. Let us define a singular surface

$$\mathbb{S}_{\mathcal{H}} \subset X.$$

Let D be a colored polyhedron. Pick an internal point $c_D \in D$. The cone over the 1-skeleton of D with the vertex at c_D is the *singular surface* $\mathbb{S}_D \subset D$.

Definition 4.1. *The singular surface $\mathbb{S}_{\mathcal{H}}$ is the union of surfaces \mathbb{S}_D in all colored polyhedrons:*

$$\mathbb{S}_{\mathcal{H}} := \cup_{D_{\bullet}} \mathbb{S}_{D_{\bullet}} \cup \cup_{D_{\circ}} \mathbb{S}_{D_{\circ}}.$$

Given an edge E of \mathcal{H} , there are exactly two colored polyhedrons $D_{E,\bullet}$ and $D_{E,\circ}$ sharing the edge. Their colors are different. In each of the two polyhedrons $D_{E,*}$ there is a triangle $t_{E,*}$ with the base E and the vertex at $c_{D_{E,*}}$. Denote by r_E the rectangle given by their union:

$$r_E = t_{E,\bullet} \cup t_{E,\circ}.$$

The singular surfaces $\mathbb{S}_{\mathcal{H}}$ are 2d analogs of bipartite ribbon graphs.

The points c_D and rectangles r_E are the analogs of vertices and edges of a bipartite graph.

4.0.2 Cooriented zig-zag surfaces for an alternating diagram \mathcal{H} .

For each face f of a colored polyhedron D , consider the cone $C_{D,f}$ over f with the vertex c_D . The polyhedral surface $\gamma_{D,f}$ is the boundary of $C_{D,f}$. It is the cone over ∂f . A coorientation of $\gamma_{D,f}$ is a coorientation of the surface obtained by smoothifying its corners, see Figure 26. We coorient the surface

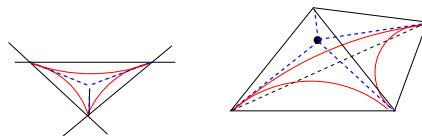


Figure 26: Smoothified strands/surfaces $\gamma_{D,i}$ (red) in a triangle/simplex.

$\gamma_{D,f}$ inside of the cone $C_{D,f}$ if D is \circ -polyhedron, and outside if D is \bullet -polyhedron.

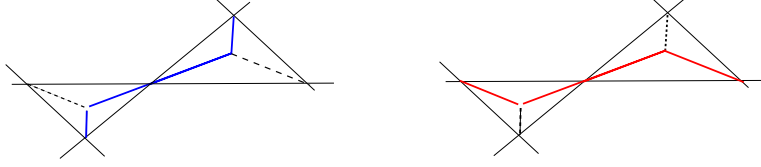


Figure 27: The two zig-zag strands, colored in blue and red, sharing a common edge.

For each of the two triangles $t_{E,*}$ sharing an E of \mathcal{H} , where $* = \circ, \bullet$, there are two surfaces γ_{D_*,f_1} and γ_{D_*,f_2} containing the cone. Here f_1, f_2 are the two faces of $D_{E,*}$ sharing E . Each of the two surfaces $\gamma_{D_\circ,f}$ can be connected to just one of the two surfaces $\gamma_{D_\bullet,f}$ so that they form a cooriented disc, see Figure 27 for the 2d analog. This way each disc extends to the unique cooriented polygonal surface γ , which we call a *zig-zag surface*.

Zig-zag surfaces are analogs of zig-zag strands of a bipartite graph Γ .

4.0.3 The spectral cover.

Assume that each zig-zag surface γ cuts M into two domains. For just one of them, denoted by \mathbb{D}_γ , the "inside the domain" boundary coorientation match the coorientation of γ . Take a copy \mathcal{D}_γ of the domain \mathbb{D}_γ . Then the disjoint union of all domains \mathcal{D}_γ projects tautologically onto M , so that each domain \mathcal{D}_γ maps to its copy \mathbb{D}_γ in M :

$$\coprod_{\gamma} \mathcal{D}_\gamma \longrightarrow M.$$

We glue the domains \mathcal{D}_γ and $\mathcal{D}_{\gamma'}$ if their projections share a rectangle r_E , getting the *spectral space* $\overline{\Sigma}_{\mathcal{H}}$:

$$\overline{\Sigma}_{\mathcal{H}} := \frac{\coprod_{\gamma} \mathcal{D}_\gamma}{\text{gluing domains } \mathcal{D}_\gamma \text{ and } \mathcal{D}_{\gamma'} \text{ along the rectangle } r_E}. \quad (91)$$

Then there is the canonical map, which identifies the domain \mathcal{D}_γ to the one \mathbb{D}_γ :

$$\overline{\Sigma}_{\mathcal{H}} \longrightarrow M. \quad (92)$$

Definition 4.2. *An alternating diagram is called ideal if there are special points $\{s_i\}$ on the boundary of M such that for each zig-zag surface γ , the domain \mathbb{D}_γ is a (semi-)ball containing just one special point.*

If $\dim M = 2$, we recover the ideal webs [G]. Consider the *spectral threefold*

$$\Sigma_{\mathcal{H}} := \overline{\Sigma}_{\mathcal{H}} - \{\text{singular points}\}.$$

It generalises the spectral surface Σ_{Γ} assigned to a bipartite ribbon graph Γ in [GKe]. Note that the spectral surface is smooth, while the space $\overline{\Sigma}_{\mathcal{H}}$ is singular. The map (92) induces the *spectral cover* map

$$\pi_{\mathcal{H}} : \Sigma_{\mathcal{H}} \longrightarrow M_{\times}. \quad (93)$$

It generalises the spectral cover construction from [G].

Theorem 4.3. *The map (93) is ramified only over singular \bullet -edges and \bullet -vertices of $\mathcal{S}_{\mathcal{H}}$.*

For an ideal alternating diagram \mathcal{H} , the spectral threefold $\Sigma_{\mathcal{H}}$ is homeomorphic to the Lagrangian $\mathbb{L}_{\mathcal{H}}^{\circ}$.

Proof. 1. The map π is evidently unramified outside of the gluing points, and at the gluing points in the open rectangles r_E . It is unramified at the \circ -vertices and \circ -edges in the \circ -domains. Indeed, the domains \mathbb{D}_γ sharing a \circ -vertex or a \circ -edge cover each nearby point just once, see Figure 28: near a \circ -point the domains \mathbb{D}_γ are the cones $C_{D_\circ,f}$, which cover the polyhedron D_\circ .



Figure 28: The polyhedron D_\circ is the union of blue domains $\mathbb{D}_\gamma \cap D_\circ$.

The map π is ramified over the \bullet -vertices and \bullet -edges. Indeed, near a \bullet -vertex, the domains \mathbb{D}_γ are the complements to the cones $C_{D_\bullet, f}$. Therefore the ramification index at a \bullet -vertex c_{D_\bullet} is equal to the $\#(\text{faces of } D_\bullet) - 1$. Similarly, the ramification index at the \bullet -edge over a vertex v of D_\bullet is equal to the $\#(\text{faces of } D_\bullet \text{ meeting at } v) - 1$.

The domains \mathcal{D}_γ are smooth. So the singularities of $\Sigma_{\mathcal{H}}$ are contained in the set of glued points. Clearly the points where we glue two domains over an open rectangle r_E° are smooth. It is easy to see that the points on the open parts of the segments connecting the point c_D with vertices of a polyhedron D are smooth. A simple local analysis, using the description of domains \mathbb{D}_γ near the point c_D as the cones $C_{D, f}$ or their complements, shows that the points c_D are smooth as well. So $\Sigma_{\mathcal{H}}$ can be singular only at the points corresponding to the triple intersection points of \mathcal{H} . The rest follows from Lemma 4.5.

2. Since the alternating diagram \mathcal{H} is ideal, the conormal bundle T_γ^*M to the cooriented zig zag surface γ is homeomorphic to the punctured domain \mathbb{D}_γ° . Let us isotope zig-zag surfaces $\gamma \rightarrow \gamma'$ by pushing the cone boundaries $\partial C_{D, f}$ towards the corresponding face f . Then γ' is just the corresponding surface H_i of \mathcal{H} . Adding back the cones $C_{D, f}$ we recover the domains \mathbb{D}_γ° . But since $D = \cup_f C_{D, f}$, where the union is over all faces f of D , adding all these cones is equivalent to gluing the zero sections of T^*D for all colored domains D . □

Since the map $\pi_{\mathcal{H}}$ is a cover map in codimension ≤ 2 , the number of points in the generic fiber is the same. It is called the *degree* of the map $\pi_{\mathcal{H}}$. It is an invariant of a diagram, called *the rank*.

4.0.4 Singularities of the Lagrangian $\mathbb{L}_{\mathcal{H}}^\circ$ assigned to an alternating diagram in M

Lemma 4.4. *Let \mathcal{H} be an alternating diagram in a threefold M . Then the Lagrangian $\mathbb{L}_{\mathcal{H}}^\circ$ is singular. Its singularities t_\circ are the zero covectors $0 \in T_t^*M$ at the triple intersection points t of \mathcal{H} . A small ball around p_\circ is homeomorphic to a cone over a pair of pants.*

Proof. Given a triple intersection point t , take a little sphere in T^*X containing $0 \in T_t^*X$. Its intersection with $\mathbb{L}_{\mathcal{H}}^\circ$ is obtained by gluing two triangles τ_\bullet and τ_\circ , provided by the intersection with the zero sections over the \bullet and \circ domains sharing the point p , with three discs provided by the conormal bundles to the surfaces intersecting at t . We glue the triangles and discs as shown on Figure 29. Each disc can be viewed as a rectangle, and we glue two its opposite sides to two triangles, leaving the other two sides untouched. We get a sphere with three holes. Each hole is a bigon whose sides are unglued sides of the rectangles. □

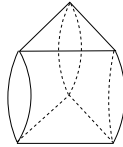


Figure 29: For an alternating diagram \mathcal{H} in a threefold, the Lagrangian $\mathbb{L}_{\mathcal{H}}^\circ$ near a singular point is a cone over a pair of pants.

Lemma 4.5. *The point $t' \in \overline{\Sigma}_{\mathcal{H}}$ corresponding to a triple intersection point $t \in M$ is singular. A small ball around p' is homeomorphic to a cone over a pair of pants. Therefore $\overline{\Sigma}_{\mathcal{H}}$ is a space with boundary.*

Proof. A neighborhood of a point t' is homeomorphic to a neighborhood of the Lagrangian $\mathbb{L}_{\mathcal{H}}^{\circ}$ near the point $0 \in T_t^*M$. The singularities of the Lagrangian $\mathbb{L}_{\mathcal{H}}^{\circ}$ were described in Lemma 4.4. \square

4.0.5 Spectral threefolds associated with \mathcal{Q} -digrams.

Given a \mathcal{Q} -diagram \mathcal{Q} in a threefold M , let us resolve its quadruple intersection points, getting an alternating diagram \mathcal{H} . Then there is the spectral space $\Sigma_{\mathcal{H}}$ and the spectral cover map (93).

Cutting out little balls B_{\bullet} surrounding the \bullet -tetrahedra in \mathcal{H} arising from the quadruple intersection points in \mathcal{Q} , we get a threefold with boundary M_{\times} . Let $p : T^*M \rightarrow M$ be the canonical projection. Set

$$\Sigma_{\mathcal{Q}} := \Sigma_{\mathcal{H}} \cap p^{-1}(M_{\times}).$$

We call $\Sigma_{\mathcal{Q}}$ the *spectral threefold assigned to \mathcal{Q}* .

Lemma 4.6. *The spectral threefold $\Sigma_{\mathcal{Q}}$ is a smooth threefold with boundary.*

If \mathcal{Q} is an ideal diagram, the spectral threefold $\Sigma_{\mathcal{Q}}$ is homeomorphic to the Lagrangian $\mathbb{L}_{\times}^{\circ}$:

$$\Sigma_{\mathcal{Q}} = \mathbb{L}_{\times}^{\circ}.$$

Proof. The first claim follows from Lemma 1.20. The second follows from Theorem 4.3. \square

If \mathcal{Q} is ideal, the projection $T^*M \rightarrow M$ induces a projection of the spectral threefold to M :

$$\pi_{\mathcal{Q}} : \Sigma_{\mathcal{Q}} \rightarrow M_{\times}. \quad (94)$$

It is called the *spectral cover map*.

5 Cluster Lagrangians in non-commutative character varieties

5.1 Two flavors of cluster varieties from \mathcal{Q} -diagrams of discs

5.1.1 Cluster varieties from alternating diagrams \mathcal{T} on a surface

Given such a \mathcal{T} , there is the stack $\mathcal{A}_{[\mathcal{T}]}$ with Zariski open substack:

$$\mathcal{A}_{\mathcal{T}}^{\circ} \subset \mathcal{A}_{[\mathcal{T}]}. \quad (95)$$

Next, there is the substack $\mathcal{U}_{[\mathcal{T}]} \subset \mathcal{X}_{[\mathcal{T}]}$ of sheaves with *trivial* rank one microlocalization at the conormal bundles to the strands of \mathcal{T} . It has a substack $\mathcal{U}_{\mathcal{T}}^{\circ} \subset \mathcal{U}_{[\mathcal{T}]}$ of the sheaves vanishing on mixed domains. These substacks are non-commutative tori.

The collections of the tori $\{\mathcal{A}_{\mathcal{T}}^{\circ}\}$ and $\{\mathcal{U}_{\mathcal{T}}^{\circ}\}$, assigned to alternating diagrams in the given admissible deformation class, provide non-commutative cluster varieties structures of two types [GKo]:

The stack $\mathcal{A}_{[\mathcal{T}]}$ is a non-commutative cluster \mathcal{A} -variety, equipped with the canonical 2-form $\Omega_{\mathcal{A}}$.

The stack $\mathcal{U}_{[\mathcal{T}]}$ is a non-commutative cluster symplectic variety with the symplectic form Ω .

Recall the groupoid $\text{Loc}_1(\Sigma_{\mathcal{T}})$ of flat line bundles on the compactified spectral surface $\Sigma_{\mathcal{T}}$. One has

$$\mathcal{U}_{\mathcal{T}}^{\circ} = \text{Loc}_1(\Sigma_{\mathcal{T}}). \quad (96)$$

Let $\text{Loc}_1^{\text{triv}}(\Sigma_{\mathcal{T}})$ be the groupoid of flat line bundles on $\Sigma_{\mathcal{T}}$, trivialized at the former punctures. Then

$$\mathcal{A}_{\mathcal{T}}^{\circ} \cong \text{Loc}_1^{\text{triv}}(\Sigma_{\mathcal{T}}). \quad (97)$$

The torus $\mathcal{A}_{\mathcal{T}}^{\circ}$ carries a non-commutative 2-form $\Omega_{\mathcal{A}}$, see (130). The 2-form $\Omega_{\mathcal{A}}$ descends under the natural map $\mathcal{A}_{\mathcal{T}}^{\circ} \rightarrow \mathcal{U}_{\mathcal{T}}^{\circ}$, which forgets trivializations, to torus (96), providing a symplectic form Ω there.

5.1.2 Cluster varieties from \mathcal{Q} -diagrams of discs in a threefold

Let us now turn to \mathcal{Q} -diagrams in a threefold M .

Definition 5.1. *Given a \mathcal{Q} -diagram of cooriented discs \mathcal{Q} in a threefold M , we consider:*

- 1) *The stack $\mathcal{A}_{[\mathcal{Q}]}$ parametrising $\mathcal{F} \in \mathcal{X}_{[\mathcal{Q}]} + \underline{\text{trivializations}}$ of their microlocal support line bundles.*
- 2) *Its substack, specified by the extra condition of vanishing on mixed domains:*

$$\mathcal{A}_{\mathcal{Q}}^{\circ} \subset \mathcal{A}_{[\mathcal{Q}]}.$$
 (98)

The image of embedding (98) is Zariski open in the target. Forgetting trivializations we get projections

$$\mathcal{A}_{\mathcal{Q}}^{\circ} \longrightarrow \mathcal{X}_{\mathcal{Q}}^{\circ}, \quad \mathcal{A}_{[\mathcal{Q}]} \longrightarrow \mathcal{X}_{[\mathcal{Q}]}.$$
 (99)

They are quotients by the action of the group $\mathcal{R} := R^{\times} \{\text{surfaces of } \mathcal{Q}\}$, acting by rescaling trivializations.

Assume now that a \mathcal{Q} -diagram of cooriented discs \mathcal{Q} intersects the boundary ∂M transversally by an alternating diagram of loops \mathcal{T} . Then the restriction functor provides functors

$$\begin{aligned} \text{Res} : \mathcal{X}_{[\mathcal{Q}]} &\longrightarrow \mathcal{U}_{[\mathcal{T}]} \\ \text{Res} : \mathcal{X}_{\mathcal{Q}}^{\circ} &\longrightarrow \mathcal{U}_{\mathcal{T}}^{\circ}. \end{aligned}$$
 (100)

Indeed, since any local system on the disc is trivial, the image of the restriction functor is a sheaf with trivial microlocalization at the punctured conormal bundle to any zig-zag loop. So it lies in $\mathcal{U}_{[\mathcal{T}]}$. We set

$$\begin{aligned} \mathcal{L}_{[\mathcal{Q}]} &:= \text{Im Res}(\mathcal{X}_{[\mathcal{Q}]}) \subset \mathcal{U}_{[\mathcal{T}]} \\ \mathcal{L}_{\mathcal{Q}}^{\circ} &:= \text{Im Res}(\mathcal{X}_{\mathcal{Q}}^{\circ}) \subset \mathcal{U}_{\mathcal{T}}^{\circ} \stackrel{(96)}{=} \text{Loc}_1(\Sigma_{\mathcal{T}}). \end{aligned}$$
 (101)

There are restriction functors for the \mathcal{A} -stacks:

$$\begin{aligned} \mathcal{L}_{[\mathcal{Q}]}^{\mathcal{A}} &:= \text{Im Res}(\mathcal{A}_{[\mathcal{Q}]}) \subset \mathcal{A}_{[\mathcal{T}]} \\ \mathcal{L}_{\mathcal{Q}}^{\mathcal{A},\circ} &:= \text{Im Res}(\mathcal{A}_{\mathcal{Q}}^{\circ}) \subset \mathcal{A}_{\mathcal{T}}^{\circ} = \text{Loc}_1^{\text{triv}}(\Sigma_{\mathcal{T}}). \end{aligned}$$
 (102)

5.2 \mathcal{A} -coordinates from \mathcal{Q} -diagrams of discs

We start from the definition of the graph of singularities $\mathcal{S}_{\mathcal{Q}}$ of any \mathcal{Q} -diagram.

Definition 5.2. *The intersection points of a \mathcal{Q} -diagram of surfaces \mathcal{Q} form the graph of singularities $\mathcal{S}_{\mathcal{Q}}$. Its vertices are the quadruple intersection points, and the edges are segments of the double intersections.*

For example, the singularity graph for the basic \mathcal{Q} -diagram in the cube \mathbb{C} is given by the twelve edges connecting the center with midpoints of the cube edges. We orient the edges out of the center. The edges of the singularity graph match the cube edges. So we can think that the \mathcal{A} -coordinates for the basic \mathcal{Q} -diagram are assigned to the (unoriented) edges of the cube. So

$$\{\text{The edges of the singularity graph of the basic diagram}\} \stackrel{1:1}{\longleftrightarrow} \{\text{The cube edges}\}.$$

Any quadruple intersection point p of a \mathcal{Q} -diagram is locally diffeomorphic to the basic \mathcal{Q} -diagram. So there are 6 singular lines passing through the point p , providing 12 edges sharing p . For each pair (p, H) where $p \in H$ is a quadruple intersection point on a surface H of a \mathcal{Q} -diagram there are two triangular cones C_{\bullet}, C_{\circ} with the vertex p , see Figure 30. They are given by the other three surfaces intersecting at p . On Figure 8, these are the cones over the two triangles on the cube containing the vertices of the diagonal perpendicular to H .

We assign to the oriented edges E of the singularity graph $\mathcal{S}_{\mathcal{Q}}$ the \mathcal{A} -variables $a_E \in R^{\times}$ subject to the following relation. Let \overline{E} be the oriented edge obtained by reversing the orientation of E . Then

$$a_{\overline{E}} = a_E^{-1}.$$
 (103)

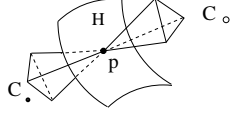


Figure 30: The two triangular cones C_\bullet, C_\circ with the vertex at the quadruple point p on the surface H .

Let us introduce a system of equations $\mathcal{R}_\mathcal{Q}$ on the \mathcal{A} -variables $\{a_E\}$. Let a, b, c be the \mathcal{A} -variables on the edges of the cone C_\bullet , oriented out of p , ordered counterclockwise, looking from the point p . For each pair (H, p) , where p is the quadruple point on the surface H of the diagram, we have the triple crossing diagram $H \cap \mathcal{Q}$ on H with a crossing point p . Let $z_1, z_2, z_3, z_4, z_5, z_6 \in R^\times$ be the \mathcal{A} -variables on the edges of the singularity graph $\mathcal{S}_\mathcal{Q}$ which lie in H , share the vertex p , and oriented out of p , see Figure 31.

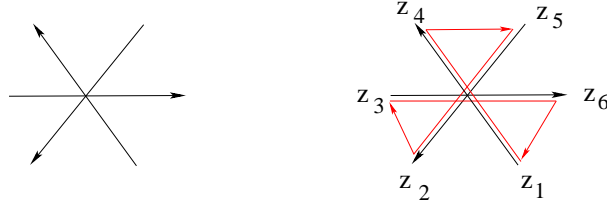


Figure 31: A triple crossing diagram and the relation $z_3 z_6 \cdot z_1 z_4 \cdot z_5 z_2 = -1$.

Definition 5.3. Let \mathcal{Q} be a \mathcal{Q} -diagram of cooriented discs in an oriented threefold. Consider the following set of equations $\mathcal{R}_\mathcal{Q}$ on \mathcal{A} -variables at the oriented edges E of the singularity graph $\mathcal{S}_\mathcal{Q}$, satisfying (103):

For each pair (H, p) , where $p \in H$ is the quadruple intersection point of \mathcal{Q} , we have:

1) For each of the two cones, C_\bullet and C_\circ , the monomial relation

$$abc = -1. \quad (104)$$

2)

$$z_1 z_4 + (z_5 z_2)^{-1} = 1, \quad z_5 z_2 + (z_3 z_6)^{-1} = 1, \quad z_3 z_6 + (z_1 z_4)^{-1} = 1. \quad (105)$$

$$z_3 z_6 \cdot z_1 z_4 \cdot z_5 z_2 = -1. \quad (106)$$

Each of the four surfaces H_i containing the quadruple intersection point p provides three equations (105). So we get twelve equations at p . By Proposition 2.9, the monomial equation (106) follows from the ones (104), and the twelve equations (105) at p are equivalent.

Theorem 5.4. Let \mathcal{Q} be a \mathcal{Q} -diagram of cooriented discs in an oriented threefold M intersecting the boundary ∂M by an alternating diagram \mathcal{T} . Then:

1. The $\mathcal{L}_{[\mathcal{Q}]}^{\mathcal{A}}$ is a non-commutative cluster Lagrangian in the cluster \mathcal{A} -variety $\mathcal{A}_{[\mathcal{T}]}$.
2. The cluster atlas for the Lagrangian $\mathcal{L}_{[\mathcal{Q}]}^{\mathcal{A}}$ is given by the Lagrangians $\mathcal{L}_{[\mathcal{Q}]}^{\mathcal{A}, \circ} \subset \text{Loc}_1^{\text{triv}}(\Sigma_{\mathcal{T}})$, where diagrams \mathcal{Q} are in the same admissible deformation class. Each of them is described by the systems of equations $\mathcal{R}_\mathcal{Q}$.
3. Similarly, $\mathcal{L}_{[\mathcal{Q}]}$ is a non-commutative cluster Lagrangian in the symplectic stack $\mathcal{U}_{[\mathcal{T}]}$.
4. In the commutative case, $\mathcal{L}_{[\mathcal{Q}]}$ is a K_2 -Lagrangian in the K_2 -cluster symplectic stack $\mathcal{U}_{[\mathcal{T}]}$.

Remark. The substacks $\mathcal{L}_{[\mathcal{Q}]}$ and $\mathcal{L}_{[\mathcal{Q}]}^{\mathcal{A}}$ can be defined for arbitrary \mathcal{Q} -diagrams. They carry \mathcal{A} -coordinates, defined below. However they are not Lagrangian if the surfaces of the diagram are not discs.

Proof. (1) Follows from Theorem 3.4.

(2) Given an object \mathcal{F} of $\mathcal{A}_{\mathcal{Q}}^{\circ}$, let us define elements $a_E \in R^{\times}$ at the oriented edges E of the singularity graph $\mathcal{S}_{\mathcal{Q}}$, called the \mathcal{A} -coordinates. Any edge E is contained in just two surfaces:

$$E \subset H_1 \cap H_2.$$

The transversal disc π_E to E contains two cooriented lines $\gamma_i := \pi_E \cap H_i$. The orientations of the edge E and the threefold M provide an orientation of the disc π_E . The lines are ordered, say h_1, h_2 , by the orientation of π_E . Consider the unique \bullet -sector $b_{h_1, h_2} \subset \pi_E$, and a path γ transporting the conormal to h_1 to the conormal to h_2 inside the sector. Denote by $\gamma(s_{H_1})$ the parallel transform of the section s_{H_1} along the path γ . We define an element $a_E \in R^{\times}$ by writing

$$\gamma(s_{H_1}) = a_E s_{H_2}.$$

The claim that the 2-form Ω vanishes on $\mathcal{L}_{\mathcal{Q}}^{\mathcal{A}, \circ}$ boils down to the calculation in [GKo, Section 6]. The subspace $\mathcal{L}_{\mathcal{Q}}^{\circ} \subset \text{Loc}_1^{\text{tr}}(\Gamma) \stackrel{(96)}{=} \mathcal{U}_{\mathcal{T}}$ is Lagrangian by (1). Therefore $\mathcal{L}_{\mathcal{Q}}^{\mathcal{A}, \circ}$ maximal isotropic.

So for each quadruple intersection point p there are 8 monomial equations (63), and equations (64).

Lemma 5.5. *Equations (63)+(64) are equivalent to the equations (36)+(35).*

Proof. Given an edge E of the graph Γ_{cube} , there are two zig-zags γ_{E-} and γ_{E+} containing the midpoint e of E . So there are two trivializations s_+ and s_- at the fiber L_e of a flat line bundle L over e . Then $s_+ = a_E s_-$, where $a_E \in R^{\times}$. The a_E is the \mathcal{A} -variable assigned to the edge E . The claim follows. \square

(3) The projection $\mathcal{A}_{[\mathcal{Q}]} \rightarrow \mathcal{U}_{[\mathcal{Q}]}$ is the quotient by the action of the group $R^{\times \{\text{surfaces of } \mathcal{Q}\}}$ by rescaling trivializations. Then (3) follows from (1) and (2).

(4) This is obvious from the general shape $x + y = 1$ of equations (105). See also Lemma 1.22. \square

5.3 \mathcal{Q} -diagrams of discs from ideal triangulations of threefolds

In Section 5.3 we consider threefolds M , possibly with boundary, glued from simplexes. Some faces of the simplexes may not belong to M . For example, take a compact threefold and remove a finite non-empty collection of points, referred to as punctures. Hyperbolic threefolds with cusps are in this category.

Given a collection of *special points* on the boundary of M , an *ideal triangulation* τ of M is a triangulation with the vertices at these points. Given an integer $m \geq 2$ and an ideal triangulation τ of a threefold M , we define an ideal \mathcal{Q} -diagram $\mathcal{Q}_{\tau, m}$ in M . It provides a singular surface

$$\mathbb{S}_{\tau, m} \subset M.$$

The construction from Section 4.0.5 assigns to the \mathcal{Q} -diagram $\mathcal{Q}_{\tau, m}$ the $m : 1$ spectral cover:

$$\pi : \Sigma_{\tau, m}^{\times} \rightarrow M^{\times}, \tag{107}$$

as well as its completion over the singular points $\pi : \Sigma_{\tau, m} \rightarrow M$.

5.3.1 Hypersimplicial decompositions.

Given a pair of integers $p, q \geq 0$, the hypersimplex $\Delta^{p,q}$ is a polyhedron of the dimension $p+q+1$, defined as an integral hyperplane section of the unit cube:

$$\Delta^{p,q} := \{x \in \mathbb{R}^{p+q+2} \mid x_0 + \dots + x_{p+q+1} = p+1, \quad 0 \leq x_i \leq 1\}.$$

So $\Delta^{0,0}$ is a segment; $\Delta^{0,1}$ and $\Delta^{1,0}$ are triangles; $\Delta^{2,0}$ and $\Delta^{0,2}$ are tetrahedra, and $\Delta^{1,1}$ is an octahedron.

The boundary of the hypersimplex $\Delta^{p,q}$ is the union of $p+q+2$ hypersimplices of type $\Delta^{p-1,q}$ and $p+q+2$ hypersimplices of type $\Delta^{p,q-1}$. It is obtained by setting one of the coordinates x_i to 0 or 1.¹²

Examples. 1. The boundary of the simplex $\Delta^{n,0}$ consists of $n+1$ simplices of type $\Delta^{n-1,0}$.

2. The boundary of the octahedron $\Delta^{1,1}$ consists of the four $\Delta^{1,0}$ -triangles, called \circ -triangles, and four $\Delta^{0,1}$ -triangles, called \bullet -triangles. Each boundary triangle shares its edges with triangles of different type. For the octahedron on Figure (35) the \bullet -triangles are on the faces of the tetrahedron.

Given integers $d \geq 1$, $m \geq 2$, take the hyperplane section of the positive cone in \mathbb{R}^{d+1} :

$$T_d := \{x \in \mathbb{R}^{d+1} \mid x_0 + \dots + x_d = m, \quad x_i \geq 0\}. \quad (108)$$

The *hypersimplicial decomposition* $\mathcal{H}_{T_d,m}$ of the simplex T_d in (108) is given by the $d+1$ families of $m-1$ hyperplanes parallel to one of the faces, defined by the equations $x_i = 1, \dots, m-1$. It cuts the simplex $T_{d,m}$ into hypersimplices of type $\Delta^{p,q}$ where $p+q = d-1$.

Examples. 1. If $d = 2$ we get an m -decomposition of a triangle into looking up and down triangles.

2. The $d = 3$ case. We consider the tetrahedron

$$T := \{x \in \mathbb{R}^4 \mid x_0 + x_1 + x_2 + x_3 = m, \quad x_i \geq 0\}, \quad m \geq 2. \quad (109)$$

The *hypersimplicial decomposition* $\mathcal{H}_{T,m}$ cuts the tetrahedron T into $\Delta^{2,0}$ -tetrahedra (looking up), octahedra $\Delta^{1,1}$, and $\Delta^{0,2}$ -tetrahedra (looking down), see Figure 32.

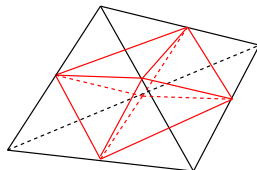


Figure 32: The hypersimplicial decomposition $\mathcal{H}_{T,2}$ of a tetrahedron into four $\Delta^{2,0}$ -tetrahedra and an octahedron.

Definition 5.6. Given an integer $m \geq 2$ and an ideal triangulation τ of a manifold X , the *hypersimplicial decomposition* $\mathcal{H}_{\tau,m}$ of X is the union of hypersimplicial decompositions $\mathcal{H}_{T,m}$ of each simplex T of τ :

$$X = \mathcal{H}_{\tau,m} = \cup_{T \in \tau} \mathcal{H}_{T,m}. \quad (110)$$

5.3.2 The singular hypersurface $\mathbb{S}_{\tau,m} \subset X$.

We define inductively a singular polyhedral hypersurface

$$\mathbb{S}^{p,q} \subset \Delta^{p,q}.$$

The point $\mathbb{S}^{0,0}$ is the center of the segment $\Delta^{0,0}$.

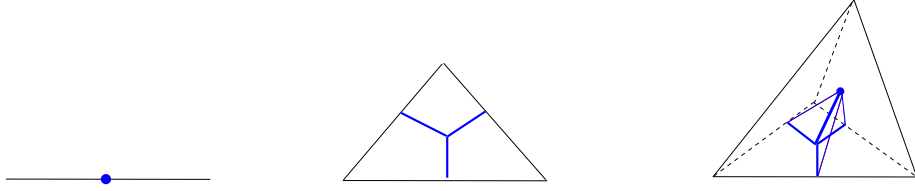


Figure 33: The point $\mathbb{S}^{0,0}$. The singular graph $\mathbb{S}^{1,0}$. A quarter of the singular surface $\mathbb{S}^{2,0}$.

Definition 5.7. *The hypersurface $\mathbb{S}^{p,q}$ is the cone over hypersurfaces $\mathbb{S}^{p-1,q}$ and $\mathbb{S}^{p,q-1}$ in the boundary hypersimplices, centered at the center of $\Delta^{p,q}$, see Figures 33, 34.*

Definition 5.8. *Given an integer $m \geq 2$ and an ideal triangulation τ of X , the singular hypersurface*

$$\mathbb{S}_{\tau,m} \subset X$$

is the union of singular hypersurfaces $\mathbb{S}^{p,q}$ in the hypersimplices of hypersimplicial decomposition (110).

The singular hypersurfaces $\mathbb{S}^{p,q}$ fit together since they induce on each of the faces of the hypersimplicial decomposition the same singular hypersurface.

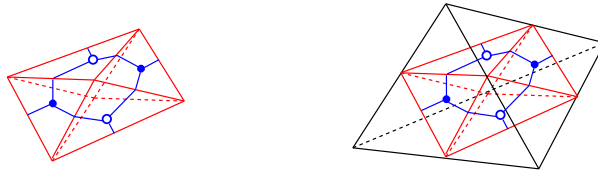


Figure 34: The surface $\mathbb{S}^{1,1}$ in the octahedron is the cone over the bipartite graph on its boundary.

When X is a surface S , the surface graph $\mathbb{S}_{\tau,m}$ is the bipartite graph $\Gamma_m \subset S$ assigned to an integer $m \geq 2$ and a triangulation of a surface in [G].

The singular hypersurfaces $\mathbb{S}_{\tau,m} \subset X$ are higher dimensional analogs of bipartite graphs.

Let us elaborate the case when X is a threefold M .

5.3.3 Hypersimplicial decompositions of a threefold.

The *hypersimplicial decomposition* $\mathcal{H}_{\tau,m}$ of a threefold M consists of the octahedra O_p , the tetrahedra t_\circ , which are $\Delta^{2,0}$ -hypersimplices, and the tetrahedra t_\bullet , which are $\Delta^{0,2}$ -hypersimplices:

$$M = \cup_p O_p \cup_\bullet t_\bullet \cup_\circ t_\circ. \quad (111)$$

The tetrahedra are glued to the octahedra. The colors of triangles are consistent: a \bullet -triangle of a tetrahedron is glued to a \bullet -triangle of the octahedron, and the same for the \circ -triangles. The octahedrons O_p correspond to the quadruple intersection points p of the \mathcal{Q} -diagram $\mathcal{Q}_{T,m}$.

5.3.4 The singular surface $\mathbb{S}_{\tau,m} \subset M$.

Singular surfaces $\mathbb{S}^{2,0} / \mathbb{S}^{0,2}$ are obtained by connecting the center of the tetrahedron with the graphs on its faces, see Figure 33. The edges of the singular locus of surfaces $\mathbb{S}^{0,2} / \mathbb{S}^{2,0}$ are called the singular \bullet -edges / \circ -edges. The centers of the tetrahedra $\mathbb{S}^{0,2} / \mathbb{S}^{2,0}$ are called the singular \bullet -vertices / \circ -vertices.

¹²Note that $\Delta^{-1,q}$ and $\Delta^{p,-1}$ are the empty sets.

The surface $\mathbb{S}^{1,1} \subset \Delta^{1,1}$ is the cone over the bipartite graph on the boundary of the octahedron. Its singular locus is given by the four \bullet -edges connecting the center with the \bullet -vertices of the boundary triangles, and four similar \circ -edges. Given a triangulation τ of M , the singular surface $\mathbb{S}_{\tau,m} \subset M$ is the union of surfaces $\mathbb{S}^{2,0}, \mathbb{S}^{0,2}, \mathbb{S}^{1,1}$ in the hypersimplicial decomposition $\mathcal{H}_{\tau,m}$. Its singular locus consists of the \bullet -edges and \circ -edges. The endpoints of singular edges are centers of the hypersimplices of the hypersimplicial decomposition.

5.3.5 Zig-zag surfaces for the singular surface $\mathbb{S}_{\tau,m} \subset M$.

Each singular surface $\mathbb{S}^{p,q} \subset \Delta^{p,q}$, $p+q=2$, carries four cooriented *zig-zag surfaces*. Their coorientations consistent with coorientations of zig-zag strands on bicolored graphs induced on the boundary of $\Delta^{p,q}$. Precisely, they look as follows.

Zig-zag surfaces for $\mathbb{S}^{2,0} / \mathbb{S}^{0,2}$ are isotopic to hemispheres around vertices of the tetrahedra $\Delta^{2,0} / \Delta^{0,2}$. They are isotopic to a part of $\mathbb{S}^{2,0} / \mathbb{S}^{0,2}$ surrounding the vertex, and coorientated out/towards the center of $\mathbb{S}^{2,0} / \mathbb{S}^{0,2}$. Zig-zag surfaces for $\mathbb{S}^{1,1}$ described as follows. In the octahedron $\Delta^{1,1}$ on Figure 35, take the four conical surfaces in the green cube C_p given by the centered at p cones over the cooriented¹³ zig-zag hexagons $\gamma_1, \dots, \gamma_4$ on Figure 19, and expand them to the octahedron.

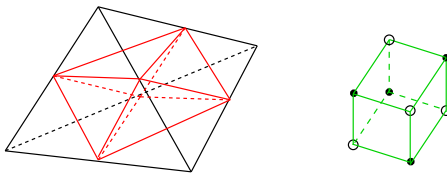


Figure 35: The green cube is inscribed into the red octahedron. Its \bullet -vertices are the centers of the octahedron \bullet -triangles - the ones on the faces of the black tetrahedron. The \circ -vertices are the centers of the octahedron \circ -triangles.

Concatenating zig-zag surfaces in the hypersimplices we get zig-zag surfaces for the hypersimplicial decomposition $\mathcal{H}_{\tau,m}$ of M . On the other hand, let us consider the \mathcal{Q} -diagram $\mathcal{Q}_{\tau,m}$.

5.3.6 The \mathcal{Q} -diagram of surfaces from an ideal triangulation of a threefold M .

Definition 5.9. The \mathcal{Q} -diagram $\mathcal{Q}_{T,m}$ is given by the following $4m$ cooriented planes in the tetrahedron (109):

$$x_i = k + \frac{1}{2}, \quad i \in \{0, 1, 2, 3\}, \quad k = 0, \dots, m-1. \quad (112)$$

Each plane is parallel to one of the faces and cooriented towards this face. The quadruple intersections q are the centers of octahedrons $\Delta^{1,1}$. They have positive half-integral coordinates, summing to m :

$$q = (q_0, q_1, q_2, q_3); \quad q_i \in \frac{1}{2} + \mathbb{Z}_{\geq 0}, \quad q_0 + q_1 + q_2 + q_3 = m.$$

The \mathcal{Q} -diagram $\mathcal{Q}_{T,m}$ cuts a standard triple crossing diagram on each face. So we can concatenate them for the tetrahedra T of an ideal triangulation τ of M , getting the \mathcal{Q} -diagram

$$\mathcal{Q}_{\tau,m} := \cup_{T \in \tau} \mathcal{Q}_{T,m} \subset M. \quad (113)$$

It gives rise to the singular surface $\mathbb{S}_{\tau,m}^{\mathcal{Q}}$.

¹³cooriented towards the \bullet vertex of the cube which is not on the zig-zag strand.

5.3.7 The two kinds of singular surfaces in threefolds coincide.

Given a triangulation τ of M , and an integer $m \geq 2$, there are two collections of singular surfaces in M :

1. The singular surface $\mathbb{S}_{\tau,m}^{\mathcal{H}}$, assigned to the m -hypersimplicial decomposition $\mathcal{H}_{\tau,m}$.
2. The singular surface $\mathbb{S}_{\tau,m}^{\mathcal{Q}}$ assigned to the \mathcal{Q} -diagram $\mathcal{Q}_{\tau,m}$ in (113).

Proposition 5.10. *The singular surfaces $\mathbb{S}_{\tau,m}^{\mathcal{H}}$ and $\mathbb{S}_{\tau,m}^{\mathcal{Q}}$ coincide, matching their zig-zag surfaces. So the related two spectral covers of M coincide.*

Proof. It is sufficient to prove this for a tetrahedron T . We claim that \bullet / \circ -domains are identified with the $\Delta^{2,0} / \Delta^{0,2}$ simplices of the hypersimplicial decomposition of T . Figure 36 shows that the intersections of singular surfaces $\mathbb{S}_{T,m}^{\mathcal{H}}$ and $\mathbb{S}_{T,m}^{\mathcal{Q}}$ with the octahedron $\Delta^{1,1}$ of the hypersimplicial decomposition coincide on the nose. Indeed, $\mathbb{S}_{T,m}^{\mathcal{Q}} \cap \Delta^{1,1}$ is the cone over the eight blue trivalent graphs with a single vertex sitting in the eight green triangles. These green triangles are the intersections of eight colored - that is \bullet or \circ - triangular cones centered at the quadruple intersection point q with the boundary of $\Delta^{1,1}$. Therefore, by the very definition, $\mathbb{S}_{T,m}^{\mathcal{H}} \cap \Delta^{1,1}$ is the cone over the same blue graphs. So we get

$$\mathbb{S}_{T,m}^{\mathcal{Q}} \cap \Delta^{1,1} = \mathbb{S}_{T,m}^{\mathcal{H}} \cap \Delta^{1,1}.$$

The claim that the intersections of singular surfaces $\mathbb{S}_{T,m}^{\mathcal{H}}$ and $\mathbb{S}_{T,m}^{\mathcal{Q}}$ with each of the tetrahedra $\Delta^{2,0} / \Delta^{0,2}$ of the hypersimplicial decomposition also coincide on the nose is clear from Figure 36 as well.

By the very definitions, this identification match the corresponding zig-zag surfaces. \square

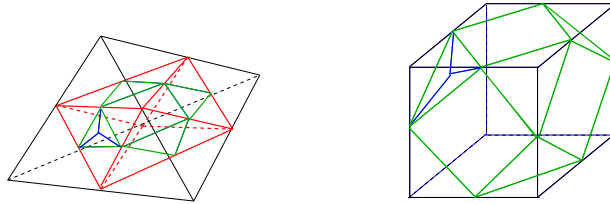


Figure 36: On the left: the red octahedron of the $m = 2$ hypersimplicial decomposition of the tetrahedron. The \mathcal{Q} -diagram with the quadruple intersection in the center cuts eight green triangles on the octahedron. On the right: the intersection of the \mathcal{Q} -diagram with a cube have eight green triangles, matching the green triangles on the left. The domains inside of the green triangles are colored.

Each zig-zag surface of $\mathbb{S}_{T,m}$ bounds a ball/halfball containing a single puncture s of ∂M , and cooriented out of the puncture. So these zig-zag surfaces form an ideal \mathcal{Q} -diagram. The spectral space $\Sigma_{T,m}$ is obtained by gluing the copies of these domains. There is a spectral map

$$\pi : \Sigma_{T,m} \longrightarrow M. \tag{114}$$

Corollary 5.11. *The spectral space $\Sigma_{\tau,m}$ is homeomorphic to the Lagrangian $\mathbb{L}_{\tau,m}^{\circ}$ associated with $\mathcal{Q}_{\tau,m}$. The spectral map π in (114) is an $m : 1$ cover map, ramified over the singular \bullet -edges and \bullet -vertices of $\mathbb{S}_{\tau,m}$. Its ramification degree is 3 at the singular \bullet -vertices of $\mathbb{S}_{\tau,m}$, and 2 over the singular \bullet -edges.*

Proof. This is a special case of Theorem 4.3. The number of domains $\mathcal{D}_{s,i}$ over a point closed to a puncture of ∂M is m . Therefore the degree of the map π is also m . \square

5.4 Cluster Lagrangians in non-commutative character varieties

5.4.1 Character varieties on surfaces of various flavors.

The stack $\mathcal{U}_m(S)$ parametrising local systems of m -dimensional R -vector spaces on a surface S with unipotent monodromies around the punctures and an invariant flag near each puncture, [FG1], [GKo].

The stack $\mathcal{A}_m(S)$ parametrises twisted m -dimensional R -local systems on S , with an invariant decorated flag near each puncture. Forgetting decorations we get a surjective map $p : \mathcal{A}_m(S) \rightarrow \mathcal{U}_m(S)$.

To fit these stacks into the general framework, recall a class of bipartite ribbon graphs Γ on S , called GL_m -graphs [G]. The collection \mathcal{T} of zig-zag loops on Γ has the following features, characterizing them:

- i) For each puncture s on S there are exactly m zig-zag loops of the collection \mathcal{T} surrounding s .
- ii) Each zig-zag loop of the collection \mathcal{T} surrounds just one puncture.
- iii) The rank of the spectral cover is equal to m , see [G] for details.

Lemma 5.12. *One has*

$$\mathcal{U}_m(S) = \mathcal{U}_{[\mathcal{T}]}, \quad \mathcal{A}_m(S) = \mathcal{A}_{[\mathcal{T}]}.$$

Lemma 5.12 explains the role of framing in the definition of the stacks $\mathcal{U}_m(S)$ and $\mathcal{A}_m(S)$.

Proof. Let S be a surface with the finite set of punctures P . Denote by \mathcal{C}_m the collection given by m concentric circles near each puncture. Then by the very definition we have a canonical equivalence

$$\mathcal{U}_{\mathcal{C}_m} = \mathcal{U}_m(S), \quad \mathcal{A}_{\mathcal{C}_m} = \mathcal{A}_m(S).$$

One can deform \mathcal{C}_m to a collection of zig-zag loops of a GL_m -graphs graph on S [G]. So the invariance of these stacks under admissible deformations proves the claim. \square

The stack $\mathcal{U}_m(S)$ carries a non-commutative cluster symplectic structure, invariant under the mapping class group Mod_S of S . Its cluster tori include the ones assigned to the GL_m -graphs on S .

5.4.2 Cluster Lagrangians in moduli spaces of non-commutative local systems on surfaces.

The stack $\mathrm{Loc}_m(S)$ of m -dimensional local systems on a closed surface S is symplectic. A threefold M with the boundary S gives rise to a Lagrangian, given by the local systems on S which extend to M :

$$\mathrm{Loc}_m(M) \subset \mathrm{Loc}_m(S).$$

This is generalized to punctured surfaces as follows. Let S be a surface with punctures, S' is the surface compactifying S , and M is a threefold with the boundary S' and a set P *special boundary points* matching the punctures on S . Let $\mathcal{L}_m(M, P)$ be the stack of non-commutative m -dimensional framed local systems on S , with unipotent monodromies around the punctures, which can be extended to M :

$$\mathcal{L}_m(M, P) \subset \mathcal{U}_m(S). \tag{115}$$

Theorem 5.13. *The substack (115) is a non-commutative cluster Lagrangian. Each ideal triangulation \mathcal{T} of M provides a system of equations $\mathcal{R}_{\mathcal{Q}, \mathcal{T}, m}$ on the variables $\{a_E\}$, describing an open part of $\mathcal{L}_m(M, P)$.*

In the commutative case we recover the main result of [DGG].

For example, let D is a ball and $S = S^2 - \{p_1, \dots, p_n\}$. Let \mathcal{F}_m be the variety of flags in an m -dimensional vector space. Then

$$\mathcal{L}_m(D, P) = \underbrace{(\mathcal{F}_m \times \dots \times \mathcal{F}_m)}_{n \text{ copies}} / \mathrm{GL}_m.$$

Indeed, any local system on the ball is trivial. So a framing is the same as n flags in a fiber over a point, obtained by parallel transporting the flags to the point, considered modulo the action of $\mathrm{GL}_m(R)$.

Note that $\mathrm{Loc}_m(D)$ is just a point. So the framing is essential.

5.4.3 Cluster description of the Lagrangian $\mathcal{L}_m(M, P)$.

We combine Lemma 5.12 with its 3d analog. Namely, we extend concentric circles of the collection \mathcal{C}_m to concentric hemi-spheres in M , getting a collection of cooriented surfaces $\mathcal{S}_m \subset M$. We get the Lagrangian

$$\mathcal{U}_{[\mathcal{S}_m]} = \mathcal{L}_{\mathcal{Q}} = \mathcal{L}_m(M, P).$$

Now Theorem 5.13 follows from Theorem 5.4 and the following crucial result.

Theorem 5.14. *One can deform \mathcal{S}_m to a \mathcal{Q} -diagram \mathcal{Q} in M , so that $\partial\mathcal{Q}$ is the collection of zig-zag loops of a GL_m -graph Γ on S .*

Proof. By the construction, each surface in the diagram $\mathcal{Q}_{\tau, m}$ contains inside just one puncture p of S , and cooriented out of the point p . So one can admissibly deform the surfaces towards the unique punctures p they contain, we get a new diagram of surfaces $\mathcal{Q}'_{\tau, m}$ such that each puncture is surrounded by exactly m surfaces. The deformation does not change the related moduli spaces. So we get an equivalence of stacks

$$\mathcal{L}_{\mathcal{Q}_{\tau, m}} \xrightarrow{\sim} \mathcal{L}_m(M, P). \quad (116)$$

Its intersection with the cluster symplectic torus $\mathrm{Loc}_1(\Sigma_{\tau, m})$ in $\mathcal{U}_{m, S}$ contains a subtorus defined by the system of equations $\mathcal{R}_{\mathcal{Q}_{\tau, m}}$. It parametrises sheaves vanishing on the mixed domains for the alternating diagram associated with the graph $\Gamma_{\tau, m}$. \square

Theorem 5.15. *Let M be a threefold with boundary S' . Let Γ be a GL_m -bipartite graph on S . Then there exists a \mathcal{Q} -diagram \mathcal{Q}_{Γ} in M inducing on the boundary the collection of the zig-zag strands of Γ .*

Proof. Take an ideal triangulation τ of M . It gives rise to the \mathcal{Q} -diagram $\mathcal{Q}_{\tau, m}$, see Section 5.3.6. The ideal triangulation τ induces an ideal triangulation τ_S of S . Let $\Gamma_{\tau, m}$ be the standard GL_m -bipartite graph on S inscribed into this triangulation [G]. The diagram $\mathcal{Q}_{\tau, m}$ induces on S the collection of zig-zag strands of the bipartite graph $\Gamma_{\tau, m}$. Now let Γ be any GL_m -bipartite graph on S . Then there exists a sequence of two by two moves of the graph Γ which transforms it to the graph $\Gamma_{\tau, m}$ [G].

Lemma 5.16. *Given any \mathcal{Q} -diagram \mathcal{Q} in M which induces on the boundary the collection \mathcal{Z}_{Γ} of zig-zag strands of a bipartite graph Γ on S , and given a two by two move $\mu : \Gamma \rightarrow \Gamma'$, there is a canonical \mathcal{Q} -diagram \mathcal{Q}' in M which induces on the boundary the collection $\mathcal{Z}_{\Gamma'}$ of zig-zag strands of a Γ' .*

Proof. Take the standard tetrahedron T with the standard collection \mathcal{Z}_T of zig-zag strands on it. A two by two move $\mu_{\alpha} : \Gamma \rightarrow \Gamma'$ is performed inside of a certain locus α on S , shown on Figure 39. The effect of the two by two move μ_{α} on the collection of zig-zag strands \mathcal{Z}_{Γ} on S can be described by gluing to S the tetrahedra T along the two faces of the tetrahedra, matching the zig-zag strands on these two faces with the ones inside of the locus α on S . Then the zig-zag strands on the other two faces of T induce the collection of zig-zag strands of Γ' inside the locus α , see Figure 22.

On the other hand, there is a canonical \mathcal{Q} -diagram \mathcal{Q}_T in T which induces the above collection of zig-zag strands on the boundary ∂T . Therefore the effect of the two by two move μ_{α} on the \mathcal{Q} -diagram \mathcal{Q} amounts to gluing to it the \mathcal{Q} -diagram \mathcal{Q}_T . The obtained \mathcal{Q} -diagram \mathcal{Q}' is the one we need. \square

Given a GL_m -graph Γ on S , there is a sequence of two by two moves which transforms it to the GL_m -graph $\Gamma_{T, m}$. Applying Lemma 5.16 to this sequence of moves we get the \mathcal{Q} -diagram \mathcal{Q}_{Γ} . \square

6 Appendices

6.1 A: Non-commutative cluster \mathcal{A} -varieties

In Section 6.1 we recall briefly some constructions from [GKo] which we use in the paper.

A *twisted* flat vector bundle over a surface S is a vector bundle over the punctured tangent bundle $TS - \{\text{zero section}\}$ which, for each $p \in S$, has the monodromy $-\mathrm{Id}$ around a loop in $T'_p S := T_p S - \{0\}$

generating $H_1(T_p^i S, \mathbb{Z})$. Take a twisted flat line bundle \mathcal{L} on an oriented surface S with boundary ∂S . Pick a vector field v tangent to the boundary of S , following the boundary orientation. A trivialization of \mathcal{L} on the boundary ∂S is given by a non-zero section of the restriction of \mathcal{L} to v .

Let Γ be a bipartite ribbon graph, and S_Γ the associated surface. The conjugate bipartite ribbon graph Γ^* provides the spectral surface $\Sigma_\Gamma := S_{\Gamma^*}$. Then $\{\text{zig-zags on } S_\Gamma\} = \{\text{boundary components of } \Sigma_\Gamma\}$. Consider the groupoid:

$$\begin{aligned} \mathcal{A}_\Gamma^\circ &:= \{\text{Twisted flat line bundles on the spectral surface } \Sigma_\Gamma, \text{ trivialized at the boundary}\} \\ &= \{\text{Twisted flat line bundles on the surface } S_\Gamma, \text{ trivialized at the zig-zag strands}\}. \end{aligned} \quad (117)$$

Let us give a coordinate description of the non-commutative tori \mathcal{A}_Γ° via the \mathcal{A} -coordinates.

Definition 6.1. *Let Γ be a ribbon graph. The \mathcal{A} -coordinates¹⁴ on Γ are the elements $\{\Delta_E \in R^\times\}$ assigned to the oriented edges E of Γ , satisfying the following monomial relations:*

- Let E be an oriented edge, and \bar{E} the same edge with the opposite orientation. Then

$$\Delta_E \Delta_{\bar{E}} = -1. \quad (118)$$

- Let E_1, \dots, E_n be the edges incident to any vertex v of Γ , oriented out of the vertex v , whose order is compatible with their cyclic order. Then

$$\Delta_{E_1} \Delta_{E_2} \dots \Delta_{E_n} = -1. \quad (119)$$

We use the name \mathcal{A} -decorated ribbon graph for a ribbon graph with a collection of \mathcal{A} -coordinates.

Given a ribbon graph Γ , the \mathcal{A} -coordinates on Γ parametrise the isomorphism classes of twisted flat line bundles on the surface S_Γ , trivialized at the boundary. Indeed, an edge E of Γ determines two faces f_E^+ and f_E^- of S_Γ . There is a canonical homotopy class of path p_E , connecting f_E^+ and f_E^- , see Figure 37. The parallel transport along the p_E acts on the trivializations s_E^\pm at the boundary components f_E^\pm ,

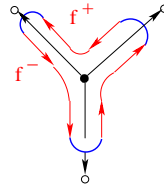


Figure 37:

defining elements $\Delta_E \in R^\times$:

$$\text{par}_{p_E} : s_E^+ \longrightarrow \Delta_E s_E^-, \quad \Delta_E \in R^\times. \quad (120)$$

Going around any edge, or any vertex along the cyclic order at this vertex, as on Figure 37, we rotate the tangent vector by 2π , getting both relations (118) and (119). The $-$ sign results from the fact that going around the circle amounts to the monodromy -1 . Conversely, a collection of the \mathcal{A} -coordinates on Γ determines a twisted flat line bundle on S_Γ .

We apply this convention to the bipartite ribbon graph Γ^* , since the twisted flat line bundles lives on S_{Γ^*} . Note that the bipartite ribbon graphs Γ and Γ^* are identical as graphs, but differs by the cyclic order of the edges in the \bullet -vertices. We depict the cyclic order on Γ as the counterclockwise, and use below the convention for the graph Γ^* in terms of the graph Γ as follows:

The counterclockwise product of the elements on the edges sharing a \circ -vertex is equal to -1 . (121)

The counterclockwise product of the elements on the edges sharing a \bullet -vertex v is $(-1)^{\text{val}(v)-1}$.

So describing twisted flat line bundles on the surface S_{Γ^*} in the terms of Γ we use convention (121).

¹⁴Calling the elements Δ_E "coordinates" is an abuse of terminology since they are not independent.

6.1.1 Two by two moves of \mathcal{A} -coordinates on bipartite ribbon graphs.

Recall the two by two move $\Gamma \rightarrow \Gamma'$ of bipartite graphs on Figure 38. Let us define the corresponding

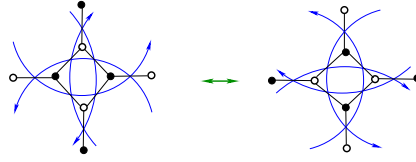


Figure 38: A two by two move of bipartite graphs.

birational isomorphism

$$\mathcal{A}_\Gamma^\circ \longrightarrow \mathcal{A}_{\Gamma'}^\circ.$$

Consider coordinates $\{a_1, a_2, a_3, a_4\}$ and $\{b_1, b_2, b_3, b_4\}$ at the internal edges on the graphs on Figure 39.



Figure 39: The two by two move of \mathcal{A} -decorated bipartite ribbon graphs is described by formulas (123).

Set

$$A_i = a_i a_{i+1} a_{i+2} a_{i+3}, \quad B_i = b_i b_{i+1} b_{i+2} b_{i+3}, \quad i \in \mathbb{Z}/4\mathbb{Z}. \quad (122)$$

Consider the following transformation of the coordinates illustrated on Figure 39.

$$\begin{aligned} b_1 &= (1 - A_3^{-1})a_3 = a_3(1 - A_4^{-1}); \\ b_2 &= (1 - A_4)^{-1}a_4 = a_4(1 - A_1)^{-1}; \end{aligned} \quad (123)$$

and the cyclic shift $i \mapsto i + 2$ of these two equations.

Note that for any $i \in \mathbb{Z}/4\mathbb{Z}$ we have $a_i A_{i+1} = A_i a_i$, $A_i = B_{i+2}^{-1}$, and

$$b_i b_{i+1} = -(a_i a_{i+1})^{-1}. \quad (124)$$

For example, $b_1 b_2 a_1 a_2 = a_3 (1 - A_4^{-1}) (1 - A_4)^{-1} a_4 a_1 a_2 = -1$. Alternatively, Figure 40 shows that formula (124) is consistent with equation (119).



Figure 40: Using conventions (119), $a_4 a_1 \alpha = -1$, $\alpha \beta = -1$, $b_4 b_1 \beta = -1$. So $a_4 a_1 = -(b_4 b_1)^{-1}$.

Proposition 6.2. [GKo] *The square of the two by two transformation (123) is the identity transformation. The coordinate transformation (123) for a two by two move satisfies the pentagon relation.*

Let us define the non-comutative cluster variety $\mathcal{A} = \mathcal{A}_{|\Gamma|}$ assigned to a bipartite ribbon graph Γ . Its clusters are parametrised by the bipartite ribbon graphs which can be obtained from Γ by two by two moves, and by shrinking two-valent vertices. We assign to each cluster the non-commutative torus \mathcal{A}_Γ , and glue them using the coordinate transformations (123) for the two by two moves. Thanks to Lemma 6.2, this definition makes sense.

6.1.2 The canonical 2-form on a non-commutative cluster \mathcal{A} -variety.

The cyclic envelope of the tensor algebra $\mathbb{T}(V)$ of a graded vector space V is a graded vector space spanned by the elements

$$\begin{aligned} v_1 v_2 \dots v_n &:= (v_1 \otimes v_2 \otimes \dots \otimes v_n)_\mathcal{C}, \\ (v_1 \otimes v_2 \otimes \dots \otimes v_n)_\mathcal{C} &= (-1)^{|v_1| \cdot (|v_2| + \dots + |v_n|)} (v_2 \otimes \dots \otimes v_n \otimes v_1)_\mathcal{C}. \end{aligned} \quad (125)$$

We define the noncommutative analog of $d \log(a_1) \wedge \dots \wedge d \log(a_n)$ by setting

$$\{a_1, \dots, a_n\} := da_1 \dots da_n a_n^{-1} \dots a_1^{-1}. \quad (126)$$

For a 3-valent ribbon graph Γ_v with a vertex v , decorated cyclically by a, b, c with $abc = \pm 1$, we set

$$\Omega_v := \{a, b\} = da db b^{-1} a^{-1}. \quad (127)$$

The condition $abc = \pm 1$ implies that it is invariant under the cyclic shift $(a, b, c) \mapsto (b, c, a)$. Note that

$$3d\{a, b\} = -(a^{-1} da)^3 - (b^{-1} db)^3 - (c^{-1} dc)^3. \quad (128)$$

Given a ribbon graph Γ_v with a single vertex v of valency > 3 , we expand this vertex by adding two-valent vertices of the opposite color, producing a bipartite ribbon graph Γ'_v with trivalent vertices of the original color, and two-valent vertices of the opposite color, and set

$$\Omega_v := \sum_{x \in \Gamma'_v} \Omega_x. \quad (129)$$

The sum is over trivalent vertices of the graph Γ'_v . It does not depend on the choice of Γ'_v .

Given an arbitrary \mathcal{A} -decorated bipartite ribbon graph Γ , we introduce the 2-form

$$\Omega_\Gamma := \sum_{w \in \Gamma} \Omega_w - \sum_{b \in \Gamma} \Omega_b. \quad (130)$$

Here the first sum is over all \circ -vertices of Γ , and the second over all \bullet -vertices.

The 2-form Ω_Γ is invariant under the two by two moves. This just means that using notation (123),

$$\{a_4, a_1\} - \{a_1, a_2\} + \{a_2, a_3\} - \{a_3, a_4\} = \{b_1, b_2\} - \{b_2, b_3\} + \{b_3, b_4\} - \{b_4, b_1\}. \quad (131)$$

We assign to each edge E of an \mathcal{A} -decorated ribbon graph Γ , decorated by an element a_E the 3-form

$$\omega_E := (a_E^{-1} da_E)^3. \quad (132)$$

Then it follows from (128) for an \mathcal{A} -decorated bipartite ribbon graph Γ , we have:

$$d\Omega_\Gamma = \sum_{E: \text{external edges of } \Gamma} \omega_E. \quad (133)$$

Theorem 6.3. *The 2-form Ω is preserved by the two by two move given by formulas (123)*

Proof. This follows from [GKo, Theorem 4.12]. Note however that formulas (123) were written in [GKo] with different sign:

$$\begin{aligned} b_1 &= (1 + A_3^{-1})a_3; & b_2 &= (1 + A_4)^{-1}a_4; \\ b_3 &= (1 + A_1^{-1})a_1; & b_4 &= (1 + A_2)^{-1}a_2. \end{aligned} \tag{134}$$

However the 2-forms do not change if we replace a_i by $-a_i$, and similarly for b_i . So changing $a_1 \mapsto -a_1, b_3 \mapsto -b_3$, and keeping the rest six variables intact we transform (134) to (123). \square

Comments on Proposition 6.2. The issue is that we use formulas (123) rather than (134). Yet the first claim follows by the same trick with the sign change as above.

6.2 B: Admissible dg-sheaves

We use the dg-enhancement of the derived category of complexes of sheaves, constructible with respect to a stratification on X from [GKo, Section 10.1]. Its objects are called dg-sheaves.

Let \mathcal{H} be a collection of cooriented hypersurfaces in a manifold X . A complex of constructible sheaves on X is \mathcal{H} -supported if its microlocal support is contained in the union of the zero section of T^*X and the conormal bundles to the cooriented hypersurfaces in \mathcal{H} .

Below we assume that the hypersurfaces in \mathcal{H} have normal crossing intersections. Among \mathcal{H} -supported dg-sheaves, we distinguish the subcategory of \mathcal{H} -admissible dg-sheaves introduced in [GKo, Section 10.1]. Below we spell the definition in the important for us cases when $\dim(X) = 2, 3$.

An \mathcal{H} -admissible dg-sheaf on a threefold M is given by the following data:

- A complex of local systems $\mathcal{F}_{\mathcal{D}}^\bullet$ on each domain \mathcal{D} of $M - \mathcal{H}$, concentrated in degrees $[0, 1]$;
- For each component γ of $\mathcal{H} - \{\text{codimension} \geq 2 \text{ strata of } \mathcal{H}\}$, sharing domains \mathcal{D}^+ , and \mathcal{D}^- and cooriented towards \mathcal{D}^+ , a map of complexes

$$\begin{aligned} \varphi_\gamma : \mathcal{F}_{\mathcal{D}^-}^\bullet &\rightarrow \mathcal{F}_{\mathcal{D}^+}^\bullet, \\ H^i \text{Cone}(\varphi_\gamma) &= 0 \text{ if } i \neq 0. \end{aligned} \tag{135}$$

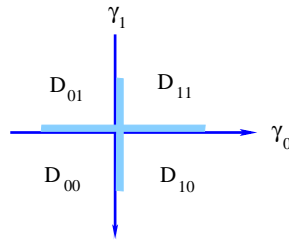


Figure 41: The stratification near a codimension two intersection of cooriented hyperplanes γ_0, γ_1 has a codimension two strata $\gamma_0 \cap \gamma_1$, four codimension one strata, and four domains \mathcal{D}_{**} .

- For each codimension two strata, given by intersection of two codimension one strata, a homotopy:

$$h : \mathcal{F}_{\mathcal{D}_{00}}^\bullet \longrightarrow \mathcal{F}_{\mathcal{D}_{11}}^\bullet[-1], \quad dh + hd = \varphi_2 \circ \varphi_1 - \varphi_4 \circ \varphi_3.$$

$$\begin{array}{ccc} \mathcal{F}_{\mathcal{D}_{01}}^\bullet & \xrightarrow{\varphi_2} & \mathcal{F}_{\mathcal{D}_{11}}^\bullet \\ \varphi_1 \uparrow & \nearrow h & \uparrow \varphi_4 \\ \mathcal{F}_{\mathcal{D}_{00}}^\bullet & \xrightarrow{\varphi_3} & \mathcal{F}_{\mathcal{D}_{10}}^\bullet \end{array} \tag{136}$$

- Similarly, for each codimension three strata, a higher homotopy

$$h_2 : \mathcal{F}_{\mathcal{D}_{000}}^\bullet \longrightarrow \mathcal{F}_{\mathcal{D}_{111}}^\bullet[-2], \quad dh_2 + h_2d = \dots$$

- Let D be the signed sum of the differentials on $\mathcal{F}_{\mathcal{D}_{***}}^\bullet$, the maps φ_* , homotopies h , and higher homotopy h_2 . Then there is the following complex, given by the direct sum of the stalks assigned to the vertices of a cube with the differential D :

$$\mathcal{F}_{\mathcal{D}_{000}}^\bullet \oplus \left(\mathcal{F}_{\mathcal{D}_{001}}^\bullet \oplus \mathcal{F}_{\mathcal{D}_{010}}^\bullet \oplus \mathcal{F}_{\mathcal{D}_{001}}^\bullet \right)[-1] \oplus \left(\mathcal{F}_{\mathcal{D}_{011}}^\bullet \oplus \mathcal{F}_{\mathcal{D}_{101}}^\bullet \oplus \mathcal{F}_{\mathcal{D}_{011}}^\bullet \right)[-2] \oplus \mathcal{F}_{\mathcal{D}_{111}}^\bullet[-3]. \quad (137)$$

We assume that this data satisfies the following condition

$$\text{Complexes (136) and (137) are acyclic.} \quad (138)$$

When X is a surface, there are no higher homotopies h_2 , and the data (137) is void.

Proposition 6.4. *Conditions (138) are equivalent to conditions that the microlocal support of \mathcal{F} does not contain any vectors in the conormal bundles to codimension two and three strata minus $\cup_i T_{H_i}^* X$, respectively.*

When X is a surface, this follows from [GKo, Lemma 10.5] and the discussion there.

The case of the threefold, involving the condition that the complex (137) is acyclic, is similar.

Precisely, given a point $q \in X$, denote by $T_{q,\mathcal{H}}^+ X$ the open cone in $T_q^* X$, given by positive linear combinations of non-zero covectors from $T_{H_i}^*$, where $q \in H_i$. Then we have the following Lemma.

Lemma 6.5. *Given an \mathcal{H} -supported complex of sheaves \mathcal{F} on X , and a codimension three stratum q of \mathcal{H} , the fiber of the microlocal support of \mathcal{F} at any $\eta \in T_{q,\mathcal{H}}^+ X$ is quasiisomorphic to complex (137).*

One easily sees, just as in Section 10 of loc. cit., that this implies the claim.

So the restriction of an \mathcal{H} -admissible dg-sheaf to the conormal bundle to each surface of \mathcal{H} is a local system. We say that a dg-sheaf has *rank one microlocal support* if these local systems, sitting in the degree zero, are one dimensional. The microlocal support on the zero section of X can be more complicated.

References

- [B] Beilinson A.: *Higher regulators and values of L-functions*, J. of Soviet Math. 30 (1985), 2036-2070.
- [BR] Berenstein A., Retakh V.: *Noncommutative marked surfaces*. [arXiv:1510.02628](#).
- [BrD1] Brav C., and Dyckerhoff T.: *Relative Calabi-Yau structures*. Compositio Mathematica 155.2 (2019), pp. 372–412.
- [BrD2] Brav C., and Dyckerhoff T.: *Relative Calabi-Yau structures II: shifted Lagrangians in the moduli of objects*. Selecta Mathematica 27.4 (2021), p. 63.
- [D] Deligne P.: *Le symbole modéré*. Publ. Mathématiques de IHÉS, Volume 73 (1991), pp. 147-181.
- [DGG] Dimofte T., Gabella M., Goncharov A.B.: *K-Decompositions and 3d Gauge Theories* [arXiv:1301.0192](#).
- [FG1] Fock V., Goncharov A.: *Moduli spaces of local systems and higher Teichmüller theory*. Publ. Math. IHES, n. 103 (2006) 1-212. [arXiv:0311149](#).
- [FG2] Fock V., Goncharov A.: *Cluster ensembles, quantization and the dilogarithm*. Ann. Sci. L'Ecole Norm. Sup. (2009). [arXiv:0311245](#).

- [FN] Freed D., Neitzke A.: *3d spectral networks and classical Chern-Simons theory*. [arXiv:2208.07420](#).
- [GPS1] Ganatra S., Pardon J., Shende V.: *Covariantly functorial wrapped floer theory on Liouville sectors*, Publ. Math. IHES 131 (2020), 73–200.
- [GPS2] Ganatra S., Pardon J., Shende V.: *Microlocal morse theory of wrapped Fukaya categories*, Ann. of Math. (2) 199 (2024), no. 3, 943–1042.
- [GPS3] Ganatra S., Pardon J., Shende V.: *Sectorial descent for wrapped Fukaya categories*, J. Amer. Math. Soc. 37 (2024), no. 2, 499–635.
- [GSV] Gekhtman M., Shapiro M., Vainshtein A., *Cluster algebras and Weil-Petersson forms* [arXiv:0309138](#).
- [G] Goncharov A.B. *Ideal webs moduli spaces of local systems, and 3d Calabi-Yau categories*. In "Algebra, Geometry, and Physics in the 21st Century". Kontsevich Festschrift. Prog. in Math., 324, 2017, p. 31-99. [arXiv:1607.05228](#).
- [GKe] Goncharov A.B., Kenyon R.: *Dimers and cluster integrable systems*. Ann. Sci. L'Ecole Norm. Sup., 2013, vol. 46, n 5, 747-813, [arXiv:1107.5588](#).
- [GKo] Goncharov A.B., Kontsevich M.: *Spectral description of non-commutative local systems on surfaces and non-commutative cluster varieties*. [arXiv:2108.04168](#).
- [GKS] Guillermou S., Kashiwara M., Schapira P.: *Sheaf Quantization of Hamiltonian Isotopies and Applications to Nondisplaceability Problems*, Duke Math J. 161 (2012) 201-245.
- [KS] Kashiwara M., P. Schapira P.: *Sheaves on Manifolds*, Grundlehren der Mathematischen Wissenschaften 292, (Springer-Verlag, 1994).
- [K] Kontsevich M.: *Symplectic geometry of homological algebra*. Arbeitstagung, Bonn, 2009.
- [N] Nadler D.: *Arboreal singularities* [arXiv:1309.4122](#).
- [STZ] Shende V., Treumann D., Williams H.: *Legendrian knots and constructible sheaves*. Inventiones mathematicae 207 (3), 1031-1133. [arXiv:1402.0490](#).
- [STWZ] Shende V., Treumann D., Williams H., Zaslow E.: *Cluster varieties from Legendrian knots*. Duke Mathematical Journal 168 (15), 2801-2871 [arXiv:1512.08942](#).
- [STW] Shende V., Treumann D., Williams H.: *On the combinatorics of exact Lagrangian surfaces*. [arXiv:1603.07449](#).
- [Th] Thurston D.: *From domino to hexagons*. [arXiv:0405482](#).